NASA TECHNICAL MEMORANDUM

NASA TM X-62,473

NASA TM X-62,473

HAZARD CRITERIA FOR WAKE VORTEX ENCOUNTERS

Robert J. Sammonds and Glen W. Stinnett, Jr.

Ames Research Center
Moffett Field, California 94035

August 1975

1. Report No.	2. Government Accession No.	3. Recipient's Catalog No.
NASA TM X-62,473		

4. Title and Subtitle	5. Report Date
HAZARD CRITERIA FOR WAKE VORTEX ENCOUNTERS	6. Performing Organization Code
7. Author(s) Robert I. Sammonds and Glen W. Stinnett, Jr.	8. Performing Organization Report No. A-6232
9. Performing Organization Name and Address Ames Research Center Moffett Field, California 94035	10. Work Unit No. 505-08-21-01 11. Contract or Grant No.
12. Sponsoring Agency Name and Address National Aeronautics and Space Administration Washington, D.C. 20546	13. Type of Report and Period Covered Technical Memorandum 14. Sponsoring Agency Code

15. Supplementary Notes

16. Abstract

A piloted, motion-base simulation was conducted to evaluate the ability of simulators to produce realistic vortex encounters and to develop criteria to define hazardous encounters for one of the several classes of aircraft of concern.

Evaluation of the simulation by pilots experienced in vortex encounters confirmed the capability of the NASA-Ames six-degree-of-freedom simulator to realistically reproduce wake vortex encounters.

A boundary for encounter hazard based on subjective pilot opinion could be identified in terms of maximum bank angle. For encounter altitudes from 200 to 500 ft (61.0 to 152.4 m), tentative hazard criteria established for visual flight conditions indicated that the acceptable upset magnitude increased nearly linearly with increasing altitude. At altitudes below 200 ft (61.0 m) and for instrument conditions, insufficient small angle encounters were obtained to establish any hazard criteria. However, the available data suggests that the allowable upsets under instrument conditions will be no greater than 50 percent of that allowable under visual conditions.

17. Key Words (Suggested by Author(s))	18. Distribution Statement
Wake vortex Wake vortex encounters Wake vortex hazard criteria Wake vortex encounter simulation	Unlimited STAR Category - 01, 03

19. Security Classif. (of this report)	20. Security Classif. (of this page)	21. No. of Pages	22. Price*
Unclassified	Unclassified	14	$3.75

*For sale by the National Technical Information Service, Springfield, Virginia 22151

NOMENCLATURE

a_x, a_y, a_z	accelerations along the x, y, z aircraft axes
c.g.	center of gravity
g	acceleration due to gravity
IFR	instrument flight rules
p, q, r	angular velocities about x, y, z aircraft axes
$\dot{p}, \dot{q}, \dot{r}$	angular accelerations about x, y, z aircraft axes
R	vortex radius
VFR	visual flight rules
x, y, z	cartesian coordinates and distances along these axes
Γ_o	vortex strength
δ_a	aileron deflection
ϵ	vortex decay effect (see eq. (1))
θ	pitch attitude
τ	vortex age (see eq. (1))
ϕ	bank angle
ψ	heading angle
$(\psi, \theta, \phi)_{w/v}$	Euler angles relating airplane wind axes to the vortex axes

HAZARD CRITERIA FOR WAKE VORTEX ENCOUNTERS

Robert I. Sammonds and Glen W. Stinnett, Jr.

Ames Research Center

SUMMARY

A piloted, motion-base simulation was conducted to evaluate the ability of simulators to produce realistic vortex encounters and to develop criteria to define hazardous encounters for one of the several classes of aircraft of concern.

Evaluation of the simulation by pilots experienced in vortex encounters confirmed the capability of the NASA-Ames six-degree-of-freedom simulator to realistically reproduce wake vortex encounters.

A boundary for encounter hazard based on subjective pilot opinion could be identified in terms of maximum bank angle. For encounter altitudes from 200 to 500 ft (61.0 to 152.4 m), tentative hazard criteria established for visual flight conditions indicated that the acceptable upset magnitude increased nearly linearly with increasing altitude. At altitudes below 200 ft (61.0 m) and for instrument conditions, insufficient small angle encounters were obtained to establish any hazard criteria. However, the available data suggests that the allowable upsets under instrument conditions will be no greater than 50 percent of that allowable under visual conditions.

INTRODUCTION

The need to increase the capacity of the nation's airports and to increase protection against accidents has led to a program by the FAA to develop an "Updated Third Generation" air traffic control system for the 1980's (ref. 1). The success of this system is dependent upon development of techniques for reducing the current longitudinal separations required to avoid the hazard from trailing wake vortices, particularly from large aircraft during approach and landing. Research on wake vortex hazard alleviation is in progress using two approaches. The first is alleviation by aerodynamic means (refs. 2-6). The second approach is to implement a wake vortex avoidance system. This system, which relies on information from ground-based measurements (refs. 3 and 6), will adjust aircraft spacings to avoid hazardous encounters when it is predicted that a vortex from a preceding aircraft is in the approach path.

As an element of the wake vortex avoidance system, research is being conducted at Ames Research Center to define criteria relating the hazard of the encounter to the response of the encountering aircraft. These criteria are being determined from a six-degree-of-freedom, moving-base, piloted simulation

which provides the means for producing a large number of repeatable encounters in an operational situation in a short period of time. The objectives of this first simulation are to (1) evaluate the ability of simulators to produce realistic encounters, (2) provide data for vortex encounter hazard criteria for one of the several classes of aircraft of concern and, (3) provide data for the development of a pilot model for use in unmanned simulations. To satisfy the first objective the Learjet was chosen as the encountering aircraft since it has been flown in a number of flight tests by pilots who were also available to participate in the simulation. This report covers the results obtained to satisfy the first two objectives. The pilot model is being developed separately by Systems Technology, Inc. under contract. This contractor was also responsible for development of the simulation model and the pilot rating scale and questionnaire for assessing wake vortex hazard.

SIMULATION

Description of the Simulator

The investigation was conducted on the NASA-Ames Research Center six-degree-of-freedom piloted-motion simulator shown in figure 1. Details pertinent to the present investigation are presented below.

Motion capabilities— The motion limits of the simulator are ±35° in roll, pitch and yaw, and ±9 ft (±2.74 m) in the longitudinal, lateral and vertical directions. Limits on rates and accelerations are given in table I. The motion logic, including washout, residual tilt, limiting circuits and cross-coupling terms is discussed briefly in Appendix A. Bode plots of frequency response for the basic simulator are also presented in Appendix A.

Cab details— The simulator is equipped with a one-man cab (fig. 1) with the instrumentation required for *VFR* and *IFR* landing approach tasks as listed in table II and shown in figure 2. The cab is equipped with throttle, gear and flap controls (fig. 3 and table III) for abort, clean-up and go-around performance. The cab is also equipped with hydraulically actuated control loaders for the wheel and column, and spring loaded pedals for the rudder controls. The hydraulic loaders were programmed to give the desired control forces and gradients with accompanying dead bands and hysteresis.

The cab was configured to approximate the Learjet used in the flight program (ref. 7) to enhance the realism to aid in evaluating the effectiveness of the simulation.

Visual and aural cues— The pilot in the cab is given visual and aural cues as well as the motion cues. The visual cues consist of a 600:1 scale landing approach scene displayed on a black and white T.V. monitor mounted above the instrument panel. When the T.V. presentation is used, the cab is completely enclosed, unlike that shown in figure 1. The visual scene is generated by a computer driven six-degree-of-freedom T.V. camera that duplicates the aircraft motion with respect to the landing approach scene.

Although the simulator motion is restricted to ±35° of bank, for example, the visual scene is capable of ±100° of bank. Thus, even though the motion cues may be restricted by physical limitations or washout terms the pilots visual scene will give realistic bank angles up to ±100°. The frequency response characteristics of the visual system are given in Appendix A.

The aural cues consist of engine noise modulated by throttle position and are introduced through stereo speakers located in the cab.

Modeling

A conventional simulation model to represent the Gates/Learjet Model 23 was developed. The forces and moments caused by encounter with the vortex were simply superimposed upon those computed for this conventional model. Representation of the vortex encounter requires a mathematical model of the vortex, and its interaction with the encountering aircraft. In addition, the simulation required special computations to ensure that repeatable encounters were obtained. Finally, turbulence was introduced that was modeled so that pilot describing function information could be derived from the measured pilot response. These modeling efforts for the wake vortex encounter simulation are described in the following paragraphs.

Aircraft model— The aerodynamic model for this simulation represents the Gates/Learjet Model 23 and includes approach and take-off configurations. The model defines the aircraft control system variables and the yaw damper and provides for clean-up and go-around following an aborted landing.

Vortex model— The vortex model is defined by a pair of two-dimensional vortices. The parameters that characterize the flow field in each case were: vortex spacing, core diameter and circulation strength. The tangential velocity from each vortex was calculated from the following equation, and the resultant velocity at a given point was computed in the manner described in reference 8.

$$|V_T| = \frac{\Gamma_o}{2\pi r}\left[1 - e^{\frac{-r^2}{4\varepsilon\tau}}\right] \qquad (1)$$

where

V_T the tangential vortex velocity

Γ_o the vortex strength (a function of the weight, speed, and wing span of the generating airplane)

ε 0.0002 Γ_o represents the vortex decay effect

τ the age of the vortex

r the radial distance from the center of the vortex

The axes of the two vortices from the generating airplane are assumed to be straight lines, and to be 84 ft (25.6 m) apart, corresponding to observed spacing for a Boeing-727 in the landing configuration.

For this particular program, 3 combinations of vortex strength and core diameter were chosen as shown in figure 4. The variation of core diameter within the range chosen has been demonstrated to have negligible effect on the calculated upset. In each case, the tangential velocity out to a radius of 35 ft (10.67 m) was determined according to equation 1 and then decreased linearly to become 0 at a radius of 70 ft (21.34 m). The objective of this truncation of the flow field was to make it impossible for the pilot to sense the presence of the vortex at greater distances and preserve the characteristic suddenness of the upsets observed in flight. The vortex properties shown in figure 4 were chosen to obtain the desired upset magnitude. No attempts were made to duplicate values characteristic of the B-727 aircraft.

Encounter geometry— The severity of the vortex upset depends not only on vortex strength, but also on the encounter conditions (i.e., how close the aircraft comes to the vortex core and the angle of the flight path relative to the vortex axis). These encounter conditions are specified in terms of a target point and an entry angle as shown in figure 5. The target point specifies how close the aircraft's initial velocity vector (aircraft *c.g.*) comes to the vortex core and the entry angle specifies the attitude of the velocity vector relative to the vortex axis. To ensure that the aircraft's center of gravity will traverse the target point and obtain repeatable encounters, the vortex origin is translated in such a manner that the aircraft's center of gravity is always heading toward the target point regardless of aircraft motions. Just prior to reaching the target point the vortex origin is frozen in inertial space. This freezing point is selected close enough to the target point to ensure that it will be encountered but distinct enough from the target point so that the pilot can change his flight path relative to the vortex once its presence is sensed. For the present simulation, the target point was always located at the center of the vortex core.

Vortex-aircraft interaction model— The forces and moments due to the presence of the vortex flow field were calculated by strip theory using the method shown in reference 8. In brief, this procedure divides the wing, horizontal tail, and vertical tail into N-number of chordwise strips. (For this case, the wing was divided into 20 strips per semi-span, while the horizontal and vertical tails were each divided into 6 strips per panel.) The local velocity, angles of attack and side slip, and forces and moments (referred to the airplane center of gravity) due to the vortex were calculated for each strip. These incremental forces and moments were summed and combined with estimated fuselage contributions to give the net forces and moments on the airplane due to the vortex.

Turbulence model— Turbulence was introduced to obtain the pilot response to a known disturbance for the development of pilot describing functions. The motions due to turbulence were considered to be equivalent to those due to aileron and elevator inputs which were added to the motions computed in response to pilot inputs. The equivalent aileron and elevator input were computed as follows:

$$\delta_j = \sum_{j=1}^{5} A_j \sin (\omega_j t + \phi_j) \tag{2}$$

where the phase (ϕ_j) was randomly selected for each run, the frequencies (ω_j) were specified in terms of number of cycles over a given time period, and the amplitudes (A_j) were specified in degrees of control surface (elevator and aileron). Numerical values of these variables are shown in table IV where

$$\omega_j = \frac{2\pi N_j}{T_{\text{run}}} \tag{3}$$

and

$$T_{\text{run}} = 25 \text{ s}$$

The amplitudes shown are for the "high" turbulence level. The "moderate" turbulence level was one-half of these values.

TEST PROGRAM

The test program was limited to vortex encounters during the landing approach. The piloting task was to fly either an *IFR* or *VFR* approach on a 3° glideslope starting with the aircraft trimmed on glideslope and localizer at the proper airspeed. The pilot was instructed to continue to a landing if possible but was given abort capability if desired (gear, flap and engine control).

Data acquisition— For each encounter the pilot was asked to assess the hazard in terms of a hazard rating scale developed for this simulation and to answer a pilot questionnaire pertaining to the encounter. The rating scale and pilot questionnaire are presented in Appendix B. The subjective pilot assessment of the vortex encounter provided the only evaluation of hazard of the encounter. In addition, those pilots who had flight experience in encountering wake vortices in the Learjet were asked to assess the realism of the simulation.

A number of response parameters such as bank angle, roll rate, altitude and control surface deflections, etc. were recorded on two 8-channel Brush recorders.

Matrix of test conditions— The test variables used for this program are given in table V. They include 3 vortex strengths (Γ_o = 1000 (92.9), 1500 (139.4) and 2000 (185.8) ft^2/s (m^2/s)), 4 encounter angles $\left(\psi_{w/v}/\theta_{w/v} = \pm 7°/0,\ \pm 15°/0,\ \pm 7°/-7°, \text{ and } \pm 10°/-10°\right)$, 5 nominal encounter altitudes (100 (30.5), 200 (61.0), 300 (91.4), 400 (121.9) and 500 (152.4) ft (m)), and 3 turbulence levels (see section on turbulence model).

Encounters were made eithe into the right or left vortex with altitude, vortex strength, and encounter angle selected in a completely random manner. In some instances, no encounter at all would be experienced. This procedure precluded the pilot predicting when an encounter might occur, how severe it would be, and its precise nature.

RESULTS AND DISCUSSION

Simulator Evaluation

Pilot subjective assessment— Four pilots were available who had extensive simulator experience and who also had had experience in intentionally encountering vortices from the B-727 and larger aircraft with the Learjet. These pilots were asked to make a subjective evaluation of the fidelity and realism of the encounters and the simulation of the Learjet.

In general, the evaluation was favorable. The pilots considered the simulation and the vortex encounters to be quite realistic and a good representation. In particular, they commented on the degree to which the encounter came as a surprise, even though it was nearly certain that the event would occur during every simulated approach.

Adverse comments, with respect to the simulation, dealt mainly with pitch and yaw motions and accelerations that were somewhat smaller than those experienced in flight. However, the primary motion, that of roll, was felt to be quite good. Some of the more abrupt or extreme encounters ran into the limitations of the simulator, in terms of either rate or travel restrictions. However, as the data were analyzed it was found that most of these encounters fell well into the hazardous regime and therefore did not contribute to the definition of the hazard boundary.

The turbulence model was felt to be quite good although it was felt that the high level of turbulence, in real life, would probably have dissipated the vortices and made an encounter unlikely.

In summary, the simulation was judged to be a useful and valid method of studying piloted vortex encounters for the purposes of establishing hazard criteria.

Comparison with flight data— Time histories of several flight encounters of the Learjet with vortices from a B-727 are presented in figure 6 for comparison with simulated encounters. (The simulation results presented are the computed aircraft motions as transmitted to the visual scene and cockpit instruments. The cab motion differs according to the motion logic described in Appendix A.) The records shown were chosen to have roughly the same maximum bank angle during the encounter. However, because of the unpredictable nature of a wake vortex encounter, it would be expected that no two time histories would match in detail. It is evident that the simulated and flight encounters are similar in that all aircraft motions were excited, and that the maximums of each motion were of the same order of magnitude.

Hazard Criteria Definition

Hazard rating— Each pilot, on completion of a run, was asked to evaluate the encounter using the rating scale and questionnaire presented in Appendix B. The rating scale was abandoned because there was no correlation between the direct assessment of hazard (question 3 of the questionnaire) and the pilots' rating from the scale. For example, there were frequent cases where an encounter was considered to be hazardous even though low numbered ratings were assigned, that is: aircraft control was not a factor, the demands on the pilot were light, and the aircraft excursions were negligible. The fourth column on the scale, in which the pilot was asked to assign a numerical rating to the hazard also correlated poorly with the direct question concerning hazard. This is believed to have been caused by a tendency of the pilots to give this rating as an average of the other three, none of which assessed hazard, per se.

It was, however, possible to accomplish an effective data correlation solely on the basis of the pilot's response to the question "Did you consider the run to be hazardous?" All encounters were therefore rated as either hazardous or non-hazardous, and a boundary was sought in terms of response parameters that segregate the data into hazardous and nonhazardous regions.

Experimental results— The data base consists of more than 200 encounters made by five pilots (see Appendix C for pilot resumes). The data were obtained for both *IFR* and *VFR* situations. However, very few of the encounters for *IFR* conditions were rated as nonhazardous, which precludes establishment of a hazard boundary for *IFR* conditions from this data set. Consequently, the detailed data analysis to establish hazard criteria was limited to the *VFR* situation.

It was anticipated that the hazard associated with a given upset during the landing approach would be strongly correlated with the altitude at which it occurred. The procedure used in correlating the data, therefore, was to plot the various response parameters in roll, pitch, yaw, normal acceleration, etc., as a function of encounter altitude and seek the parameter that best accomplishes a separation of the data into hazardous and nonhazardous regions.

Of the various parameters considered, the roll responses were thought most likely to provide the desired criterion based on observation of the relative magnitudes of the responses and the fact that roll acceleration had been found in flight to correlate well with acceptable separation distance (refs. 7, 9, and 10). In the present analysis, the parameter that yielded the best defined hazard boundary was maximum bank angle. This was chosen to be the maximum bank angle that occurred in response to the vortex and included any corrective action taken by the pilot to regain control. The correlation of the bank angle data is shown in figure 7 and includes all encounters obtained under *VFR* conditions. Those encounters assessed as hazardous by the pilots are designated by the filled symbols. The hazard boundary shown clearly separates the data into two regions: one containing no hazardous encounters; and one in which an encounter is likely to be hazardous. It is not possible to extend this hazard boundary to altitudes less than about 200 ft (61.0 m) because none of the encounters simulated at the lower altitudes were considered to be nonhazardous.

The tentative hazard boundary drawn in figure 7 appears to be reasonably representative of the opinion of all of the participating pilots in that each of them contributed at least one hazardous data point close to the boundary. However, since the upsets were generated by varying either the encounter angle or the vortex strength, the question arises as to whether the boundary determined in figure 7 is predominantly that of any one particular encounter condition. To answer this question, data are presented in figure 8 that are restricted to a single encounter angle for varying circulation strength and vice versa. In either case, the tentative hazard boundary drawn to fit all of the data (from fig. 7) also provides a reasonable boundary to the region containing the hazardous encounters from the limited data sets.

Correlation of the pilot's assessment of hazard with either roll rate or roll acceleration was considerably less successful. The correlation in terms of roll rate is shown in figure 9. While some separation of the data into hazardous and possibly hazardous regions is evident, a boundary cannot be drawn that separates as many of the nonhazardous encounters from the data set as was possible in the case of maximum bank angle.

The correlation of the pilot's assessment of hazard with roll acceleration is shown in figure 10. These results are of particular interest since, as previously mentioned, roll acceleration has been used as a correlation parameter for the flight investigations reported in references 7, 9, and 10. The parameter used in the flight program was the ratio of the vortex induced roll acceleration to the roll control power of the airplane. Since, for a given flight condition, the roll control power of the aircraft is a constant this parameter is analogous to that used in figure 10. In terms of this parameter, the nonhazardous encounters were found to be randomly distributed throughout the range of the data as illustrated in figure 10, and definition of a hazard boundary that separates a significant number of the nonhazardous encounters from the rest of the data is not possible.

As previously mentioned, the severity of the encounter was controlled by varying either the vortex strength or the encounter angle independently. The maximum bank angles obtained in this manner varied by a factor of 4 in either case (figs. 11(a) and (b)). However, only when the encounter angle was held constant (fig. 11(b)) did the maximum bank angle show any significant variation with the vortex induced roll acceleration. For this condition, the maximum bank angle tends to lie in a band, with the mean value following an approximately linear relationship with the vortex induced roll acceleration. Since the hazard assessment has been shown to correlate in terms of maximum bank angle (fig. 7), it follows that this restricted data set should also correlate in terms of the acceleration parameters. Such a correlation is shown in figure 12, and it is clear that a reasonable separation of the data into nonhazardous and possibly-hazardous regions is obtained.

It is speculated that the flight test procedures (refs. 7, 9, and 10) limited the encounter angles to a much smaller range than was covered in the simulation. If this range were sufficiently small, the simulation results demonstrate that an assessment of hazard in terms of maximum acceleration due to the vortex should provide a correlation of the data.

However, the simulation data show that the pilot's hazard assessment correlates well with maximum bank angle for a wide range of encounter angles and vortex strengths. This indicates that the pilots assessment of the hazard is based on the magnitude of the upset rather than the means in which the upset is generated.

As noted previously, the simulated vortex encounters under *IFR* conditions were, almost without exception, assessed to be hazardous (fig. 13). Pilot commentary indicates that disorientation was the primary cause for this assessment. For the *IFR* encounters, the smallest maximum bank angle at each altitude was on the order of 50 percent of the maximum bank angle defining the hazard boundary for *VFR* conditions. The hazard boundary for *IFR* conditions must therefore lie at maximum bank angles no greater than one half of those considered acceptable under *VFR* conditions.

CONCLUDING REMARKS

A preliminary simulation has been conducted to evaluate the usefulness of piloted moving-base simulation for development of hazard criteria for wake vortex encounters, and to determine this criteria for one class of aircraft.

Pilot opinion indicated that the simulation was sufficiently realistic and representative of flight encounters to be a useful tool for the establishment of hazard criteria.

Pilot evaluations of encounter hazard, for *VFR* conditions, correlated well with maximum roll attitude with the allowable upset increasing nearly linearly with increasing altitude. For altitudes below 200 ft (61.0 m) and for instrument flight conditions, insufficient data were obtained at small upset angles to establish hazard criteria. However, the available data suggests that the allowable upset under instrument conditions will be no greater than 50 percent of that allowable under visual conditions.

APPENDIX A

MOTION LOGIC AND FREQUENCY RESPONSE OF S.01 SIMULATOR

Motion logic— The S.01 motion simulator requires three velocity command signals (for the translational axes; X, Y, and Z motion of the simulator), and three rotational position command signals (for the rotational axes, ϕ, θ, and ψ motion of the simulator). A motion drive program has been designed to compute these drive signals based on acceleration and/or rate information supplied by the simulated aircraft through the solution of the equations of motion for a rigid body vehicle. The drive signals have acceleration washouts, limiting circuitry and cross coupling effects to approximate the same feel as would be felt in the simulated aircraft for the type of motion desired. This is known as the washout motion system and is shown in the block diagram in figure 14. As previously stated, the purpose of the washout motion system is to give the pilot in the simulator the feel of the simulated aircraft motions while keeping the simulator within its physical hardware limits.

The inputs to the washout motion system are the pilot station accelerations a_{x_p}, a_{y_p}, a_{z_p}, $\dot{p}_B$, $\dot{q}_B$, and $\dot{r}_B$. These quantities are normally determined in the basic computer program that solves the aircraft equations of motion. The washout system also uses the actual position feedback signal from each translational axis of the simulator. The outputs of the system are the three translational velocity drive signals and the three rotational drive signals required by the simulator.

As shown in figure 14, the acceleration inputs ($\ddot{A}_j$ and $\ddot{A}_i$) are fed into fourth order washout filters designed to pass only the high frequency components of the acceleration input. These high frequencies are important with regard to the pilots feel of the aircraft motion. The frequency (ω_{H_1} and ω_{H_2}), damping (ζ_{H_1} and ζ_{H_2}), and gain (K_1 terms) characteristics of the filter are adjusted on the basis of the particular aircraft involved and the objectives of the research program to give the desired results.

The residual tilt in figure 14(b) is provided as an additional translational acceleration cue near the end of a particular translational travel by combining the translational acceleration with the calculated simulator load factor to rotate or tilt the cab in the translational axis plane. This residual tilt is a function of ω_L and K_{LL} terms and must be accomplished at frequencies low enough so that the pilot does not sense the accompanying angular acceleration.

The high frequency false translational acceleration cues due to gravity accompanying pure cab rotation are compensated for by appropriate translational accelerations.

Additional second order filters are used (fig. 14(a)) to wash out any long-term components of the calculated acceleration ($\ddot{A}_{TS}$). These filters have

the same damping (ζ_D) and frequency (ω_D) characteristics for the washed out accelerations ($\ddot{A}_{SD}$), velocity commands ($\dot{A}_S$), and desired positions (A_S).

Calculations are also included in the motion drive program to limit the translational motion and correct for any position drift.

For this particular simulation, the roll response was improved with the addition of a second order feed forward compensation. This is given by the following equation.

$$\phi_c = \phi_\omega + 0.1515\dot{\phi} + 0.003673\ddot{\phi} \tag{A1}$$

where

ϕ_c S.01 commanded roll

ϕ_ω output of normal washout program

$\dot{\phi}, \ddot{\phi}$ computed roll rate and roll acceleration at pilot station

A listing of the S.01 motion program coefficients and values used for this simulation is presented in table VI.

Frequency response— An all digital six-axis frequency evaluation program (SAFE) has been developed to check the response characteristics of the simulator. This system drives all six axes simultaneously by a sum of sinusoids for approximately one minute. With this known input and the measured position responses, calculations are made to determine each axis' frequency response at each of the driving frequencies.

Bode plots of amplitude ratio and phase lag measured for each axis are presented in figure 15. Because the SAFE program assumes that each axis does not respond to the commands to other axis, these Bode plots are for the S.01 simulator without washout or feed forward compensation.

A similar SAFE program is also available to determine the frequency response of the visual system. Bode plots of amplitude ratio and phase lag for the visual system are presented in figure 16.

APPENDIX B

HAZARD RATING AND PILOT QUESTIONNAIRE

A multiple choice vortex hazard rating scale was developed by Systems Technology, Inc. from the results of a questionnaire distributed to some 48 private, commercial and research pilots (ref. 11). Each pilot evaluated the selectivity and sensitivity of a number of adjectives and phrases and located them on a non-adjectival scale of increasing hazard. Each pilot also graded the suitability of each adjective and phrase and specified their preference for either a Cooper-Harper style decision tree or a multiple choice format.

Analysis of these pilot evaluations resulted in the rating scale shown in figure 17. This format has columns for the evaluation of aircraft control, demands on the pilot and aircraft excursions with the selection of the adjectival phrases and their location on a scale of 1-5 being the result of the pilot survey. A fourth column was allocated to the pilots assessment of the hazard on an arbitrary scale of 1-5.

Along with the hazard rating scale, a pilot evaluation sheet or questionnaire was also used to stimulate a response from the pilot and provide answers to certain specific questions, one of which was the pilots subjective evaluation of whether the encounter was or was not a hazard. A copy of the evaluation sheet is shown in figure 18.

APPENDIX C

PILOT RESUMES

Included in this section are brief resumes of the experience and qualifications of the pilots taking part in the simulation.

Pilot A
Position: Engineering Test Pilot, NASA/Ames
Flight time:

Single engine	5850
Multi-engine	2100
Other (Hel.)	300
Total	8250

Miscellaneous: ATR

Pilot B
Position: Flight Test Pilot, FAA/NAFEC
Flight time:

Single engine	3000
Multi-engine	5500
Other	500
Total	9000

Miscellaneous: ATR

Pilot C
Position: Flight Test Pilot, FAA/NAFEC
Flight time:

Single engine	1200
Multi-engine	4500
Other	2500
Total	8200

Miscellaneous: ATR

Pilot D
Position: Aeronautical Engineer, Systems Technology, Inc.
Flight time:

Single engine	500
Multi-engine	0
Other	0
Total	500

Miscellaneous: Commercial license (ASEL) - No instrument rating

Pilot E
Position: Engineering Test Pilot, FAA/AWE-105
Flight time:

Single engine	3000
Multi-engine	8500
Other	1300
Total	12800

Miscellaneous: ATR

REFERENCES

1. Israel, D. R.: Air Traffic Control: Upgrading the Third Generation. Tech. Rev., vol. 77, no. 3, 1975, pp. 14-24.

2. Roberts, L.: On Wake Vortex Alleviation, NASA/University Conf. on Aeronautics — Theme: The Future of Aeronautics. Univ. of Kansas, Oct. 23-24, 1974.

3. Anon.: FAA Symposium on Turbulence, March 22-24, 1971, Washington, D.C.

4. McCormick, B. W.: Aircraft Wakes: A Survey of the Problem. FAA Symposium on Turbulence, March 22-24, 1971, Washington, D.C.

5. Kirkman, K. L.; Brown, C. E.; and Goodman, A.: Evaluation of Effectiveness of Various Devices for Attenuation of Trailing Vortices Based on Model Tests in a Large Towing Basin. NASA CR-2202, 1973.

6. Garodz, L. J.; Hanley, W. J.; and Miller, N. J.: Abbreviated Investigation of the Douglas DC-10 Airplane Vortex Wake Characteristics in Terminal Area Type Operations. FAA/NAFEC Project No. 214-741,04X (Special Task No. FS-2-73), Aug. 1972.

7. Barber, M. R.; Kurkowski, R. L.; Garodz, L. J.; et al.: Flight Test Investigation of the Vortex Wake Characteristics Behind A Boeing 727 During Two-Segment and Normal ILS Approaches. NASA TM X-62,398, FAA-NA-750151, 1975.

8. Johnson, W. A.; and Rediess, H. A.: Study of Control System Effectiveness in Alleviating Vortex Wake Upsets. AIAA Paper 73-833, AIAA Guidance and Control Conference, Aug. 1973.

9. Andrews, W. J.; Robinson, R. H.; and Larson, R. R.: Exploratory Flight Investigation of Aircraft Response to the Wing Vortex Wake Generated by Jet Transport Aircraft. NASA TN D-6655, 1972.

10. Robinson, G. H.; and Larson, R. R.: A Flight Evaluation of Methods for Predicting Vortex Wake Effects on Trailing Aircraft. NASA TN D-6904, 1972.

11. Hoh, R. H.: A Pilot Rating Scale for Vortex Hazard Evaluation. NASA CR-14,836, 1975.

TABLE I.— MOTION LIMITS

Motions Generated	Displacement	Acceleration	Velocity
Roll	±35°	10 rad/s^2	1.3 rad/s
Yaw	±35°	3.0 rad/s^2	3.0 rad/s
Pitch	±35°	4.5 rad/s^2	1.7 rad/s
Vertical	±9 ft (±2.7 m)	8.8 ft/s^2 (2.7 m/s^2)	7.5 ft/s (2.3 m/s)
Longitudinal	±9 ft (±2.7 m)	7.5 ft/s^2 (2.3 m/s^2)	9.0 ft/s (2.7 m/s)
Lateral	±9 ft (±2.7 m)	9.2 ft/s^2 (2.8 m/s^2)	8.0 ft/s (2.4 m/s)

TABLE II.— COCKPIT INSTRUMENTATION

Number	Instrument
1	Indicated angle of attack
2	Indicated airspeed, kt
3	Turn/Bank
4	Attitude deviation indicator
5	Horizontal situation indicator (Glide slope on right and localizer on bottom)
6	Control surface status (trim)
7	Altimeter
8	Instantaneous vertical speed indicator
9	Normal acceleration, g units
10	Clock
11	Engine RPM
12	Flap deflection
13	Gear status lights: UP, DOWN

TABLE III.— COCKPIT CONTROLS

Number	Control
1	Column and wheel
2	Pitch and roll trim (thumb switch)
3	Rudder pedals
4	Throttle levers
5	Flap handle
6	Gear handle
7	Yaw damper ON/OFF switch

TABLE IV.— NUMERICAL VALUES OF ROLL AND PITCH TURBULENCE VARIABLES

j	A_j		N_j		ω_j (rad/s)	
	Aileron	Elevator	Aileron	Elevator	Aileron	Elevator
1	0.61	0.66	2	3	0.503	0.754
2	1.22	0.90	5	7	1.257	1.759
3	3.065	1.80	12	17	3.016	4.273
4	3.065	1.37	25	31	6.283	7.791
5	3.065	1.78	41	47	10.304	11.812

TABLE V.— VORTEX ENCOUNTER CONDITIONS

Vortex strength $ft^2/s(m^2/s)$	$\psi^\circ_{\omega/v}$	$\theta^\circ_{\omega/v}$	Nominal encounter altitude, ft (m) 100 (30.5)	200 (61.0)	300 (91.4)	400 (121.9)	500 (152.4)
1500	-15	0	X	X	X	X	
(139.4)	+15	0	X	X	X	X	
1000	+10	-10	X	X	X	X	
(92.9)	-10	-10	X	X	X	X	
1000	-7	-7		X	X	X	X
(92.9)	+7	-7		X	X	X	X
1000	-7	0			X	X	X
(92.9)	+7	0			X	X	X
1500	+10	-10			X	X	X
(139.4)	-10	-10			X	X	X
2000	+10	-10				X	X
(185.8)	-10	-10				X	X

TABLE VI. S.01 MOTION PROGRAM COEFFICIENTS AND VALUES

	Symbol	Values
Washout filters	$\omega_{H_{X1}}, \omega_{H_{X2}}$	0.3, 0.3
	$\omega_{H_{Y1}}, \omega_{H_{Y2}}$	0.3, 0.3
	$\omega_{H_{Z1}}, \omega_{H_{Z2}}$	0.3, 0.3
	$\omega_{H_{P1}}, \omega_{H_{P2}}$	0.3, 0.3
	$\omega_{H_{Q1}}, \omega_{H_{Q2}}$	0.75, 0.75
	$\omega_{H_{R1}}, \omega_{H_{R2}}$	0.75, 0.75
	$\zeta_{H_{X1}}, \zeta_{H_{X2}}$	1.4, 1.4
	$\zeta_{H_{Y1}}, \zeta_{H_{Y2}}$	1.4, 1.4
	$\zeta_{H_{Z1}}, \zeta_{H_{Z2}}$	1.4, 1.4
	$\zeta_{H_{P1}}, \zeta_{H_{P2}}$	1.4, 1.4
	$\zeta_{H_{Q1}}, \zeta_{H_{Q2}}$	0.7, 0.7
	$\zeta_{H_{R1}}, \zeta_{H_{R2}}$	0.7, 0.7
	K_X, K_Y, K_Z	0.5, 0.5, 0.5
	K_P, K_Q, K_R	0.5, 0.5, 0.5
Residual Tilt	$\omega_{L_X}, \omega_{L_Y}, \omega_{L_Z}$	2., 2., 0.
	$K_{LL_X}, K_{LL_Y}, K_{LL_Z}$	1., 1., 0.

TABLE VI. S.01 MOTION PROGRAM COEFFICIENTS AND VALUES — CONCLUDED.

	Symbols	Values
Translational	$\omega_{D_X}, \omega_{D_Y}, \omega_{D_Z}$	0.2, 0.2, 0.2
	$\zeta_{D_X}, \zeta_{D_Y}, \zeta_{D_Z}$	0.707, 0.707, 0.707
	$K_{N_X}, K_{N_Y}, K_{N_Z}$	0.25, 1., 1.
	$K_{E_X}, K_{E_Y}, K_{E_Z}$	0.5, 0.5, 0.5
	$K_{O_X}, K_{O_Y}, K_{O_Z}$	1., 1., 1.
Rotational	$\omega_{E_P}, \omega_{E_Q}, \omega_{E_R}$	0.1, 0.1, 0.1
Limits	$\ddot{X}_{M_L}, \ddot{Y}_{M_L}, \ddot{Z}_{M_L}$	5.6, 6.8, 5.5
	$\dot{X}_{M_L}, \dot{Y}_{M_L}, \dot{Z}_{M_L}$	8.5, 7.5, 7.0
	$\dot{\phi}_{M_L}, \dot{\phi}_{M_L}, \dot{\phi}_{M_L}$	1.2, 1.5, 2.8
	$X_{M_L}, Y_{M_L}, Z_{M_L}$	7., 7., 7.
	$\phi_{M_L}, \phi_{M_L}, \phi_{M_L}$	0.5326, 0.5326, 0.5326

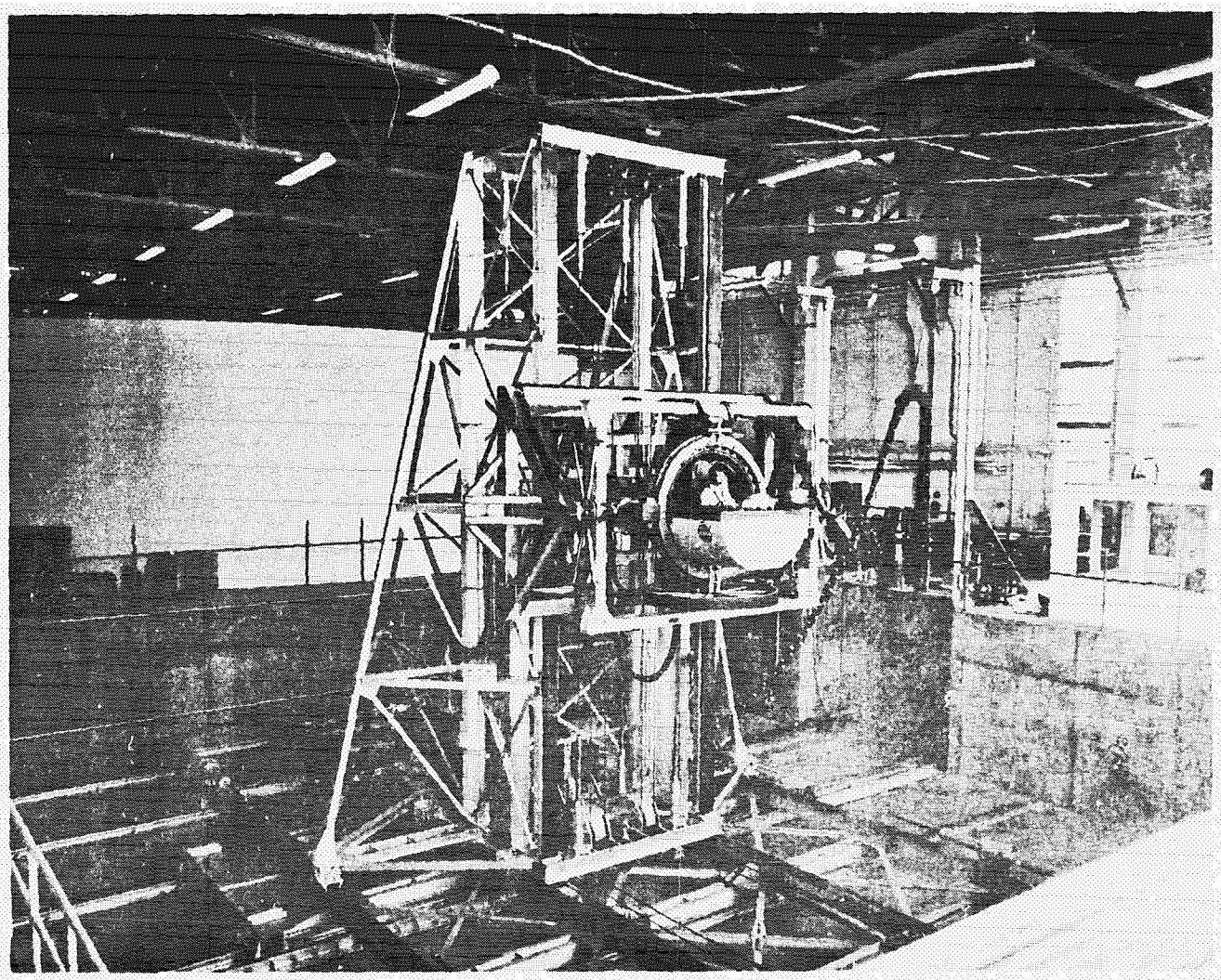

Figure 1.— Ames six-degree-of-freedom moving base simulator.

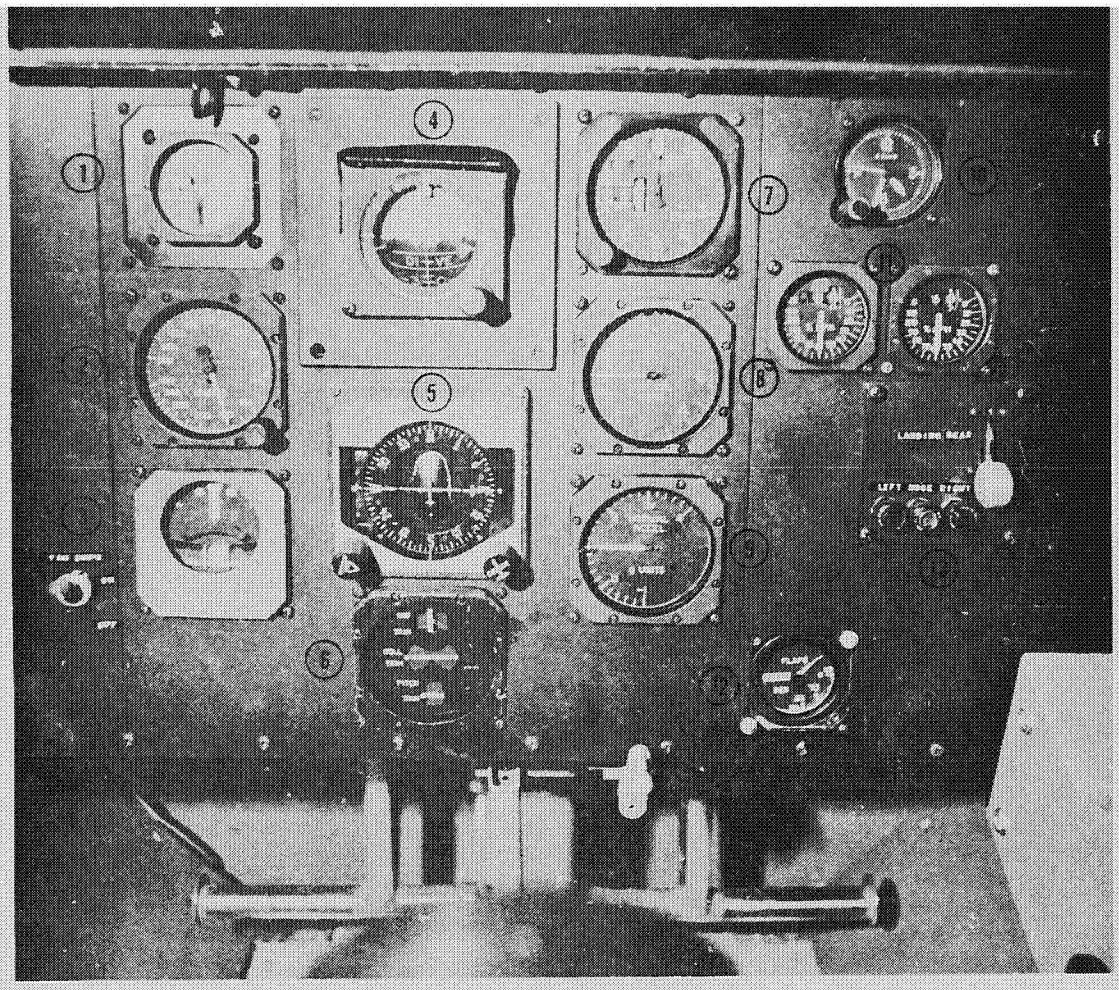

Figure 2.— Instrument panel layout (see table II for identification of instruments).

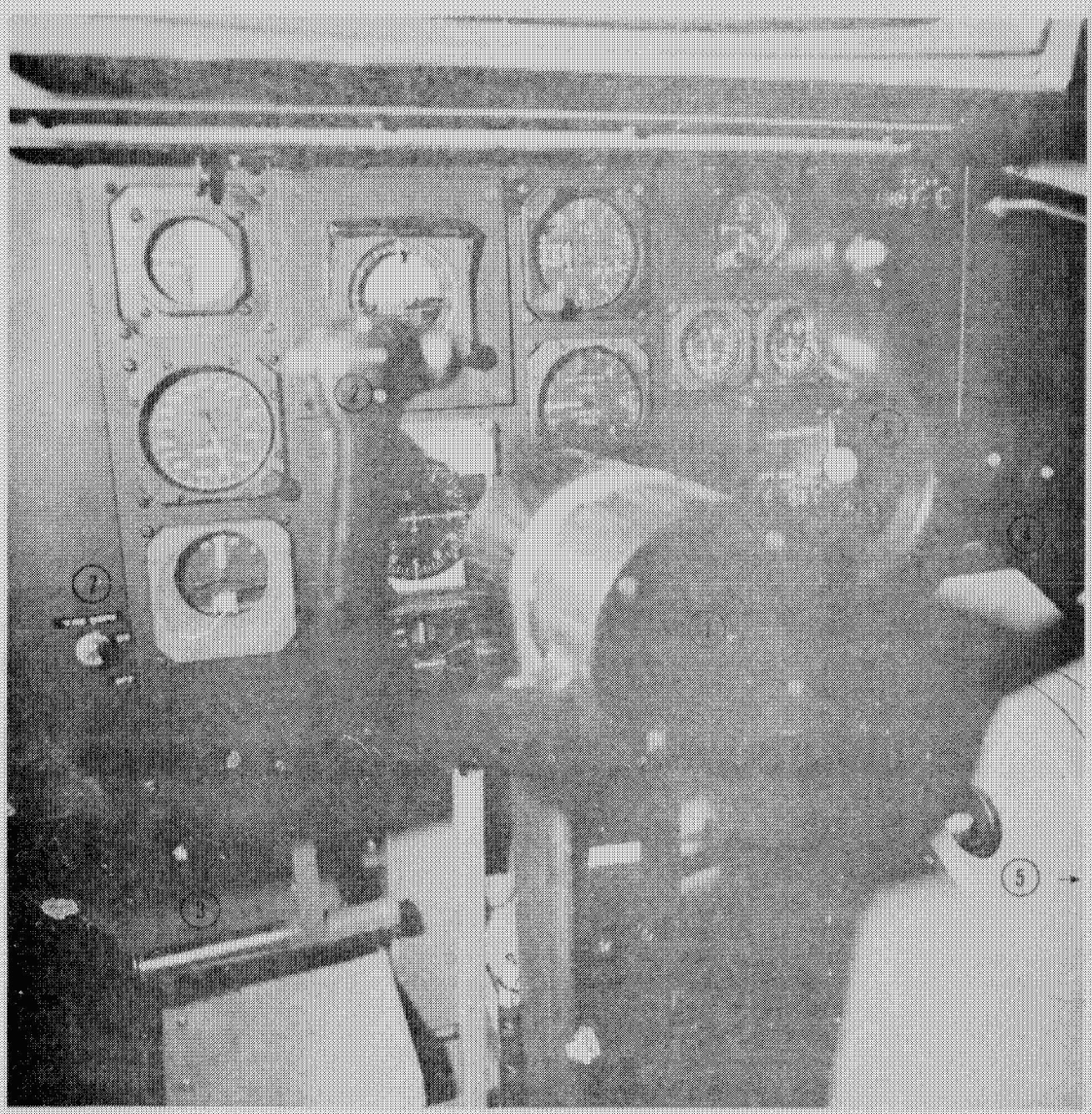

Figure 3.— Cab controls (see table III for identification of controls).

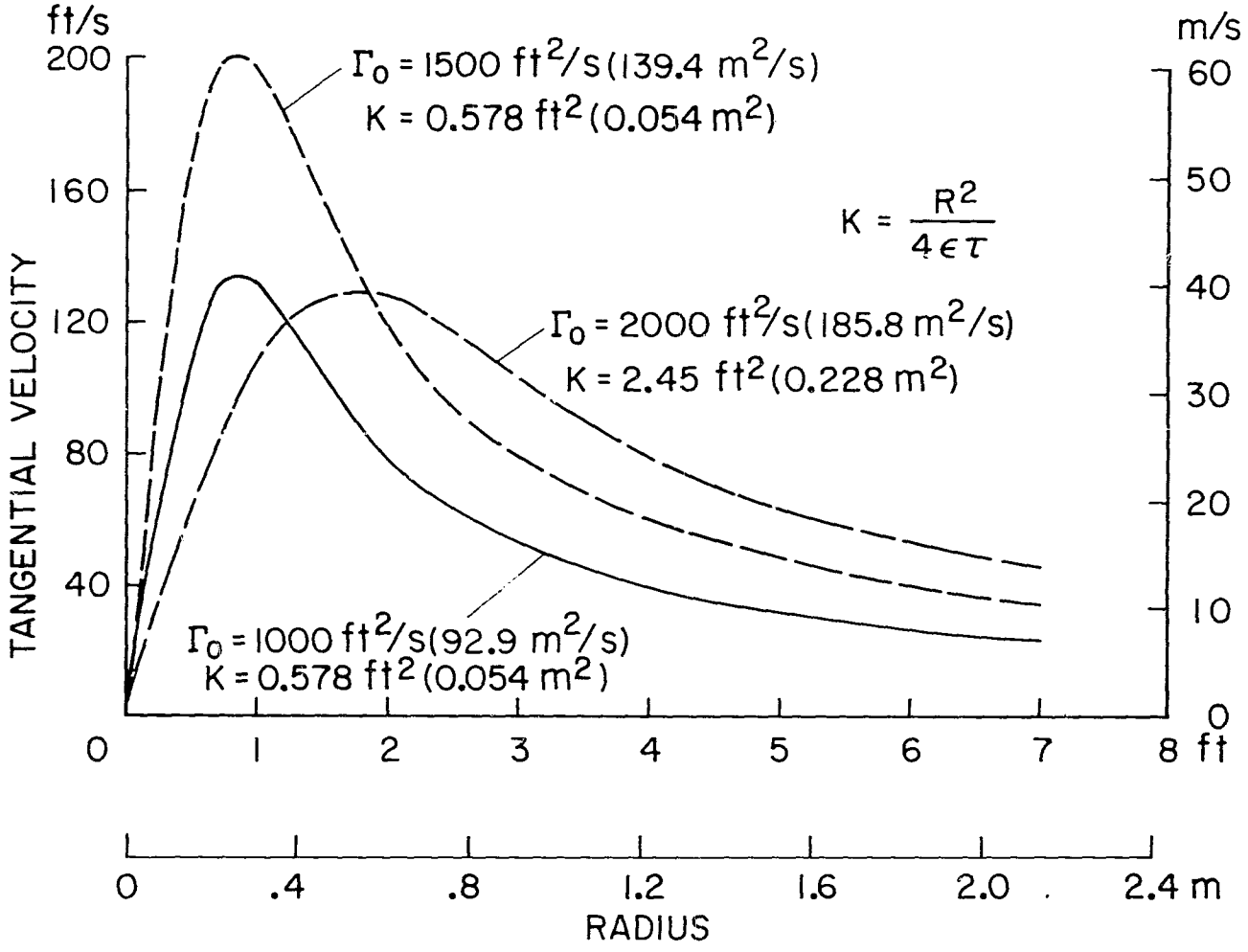

Figure 4.— Vortex models.

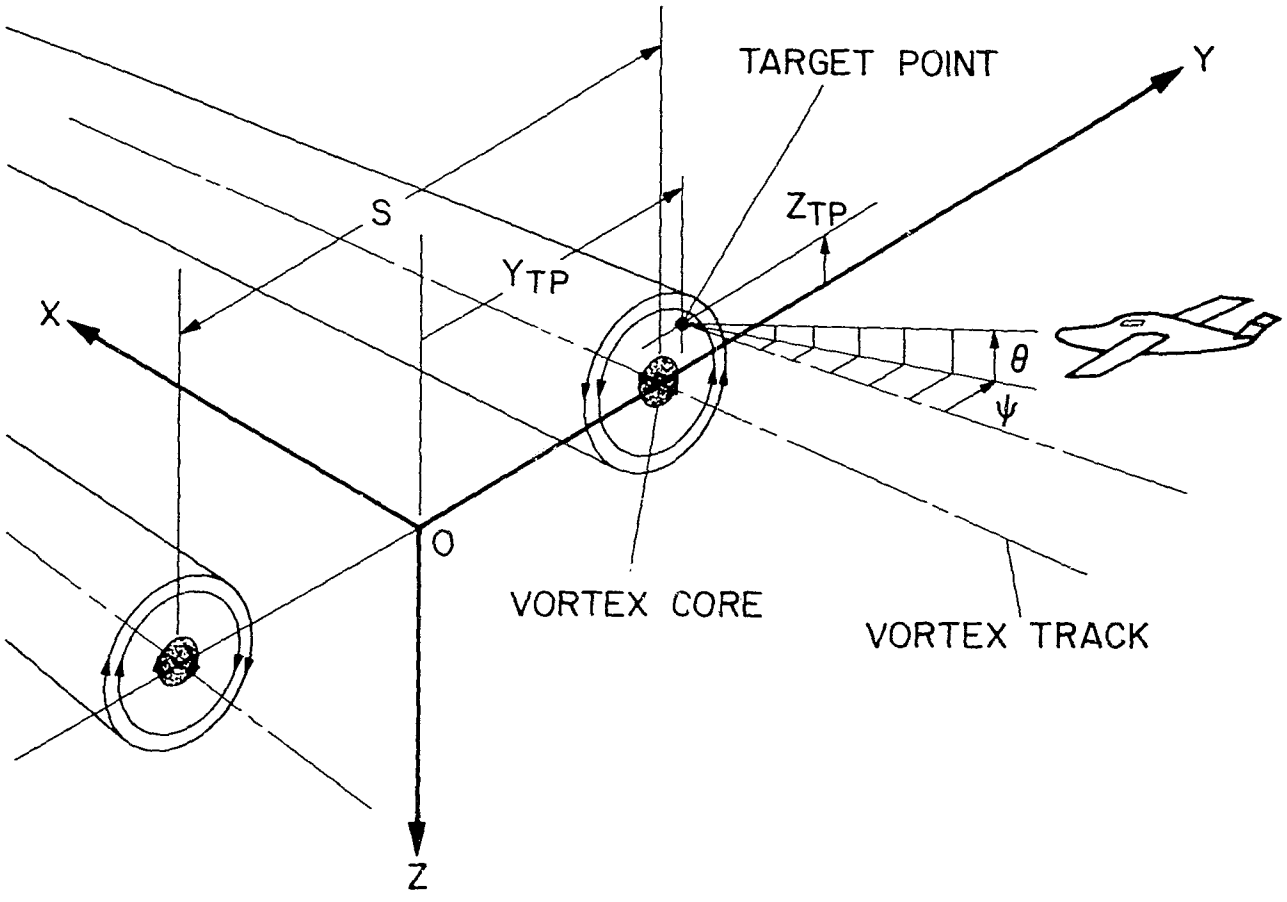

Figure 5.— Encounter geometry.

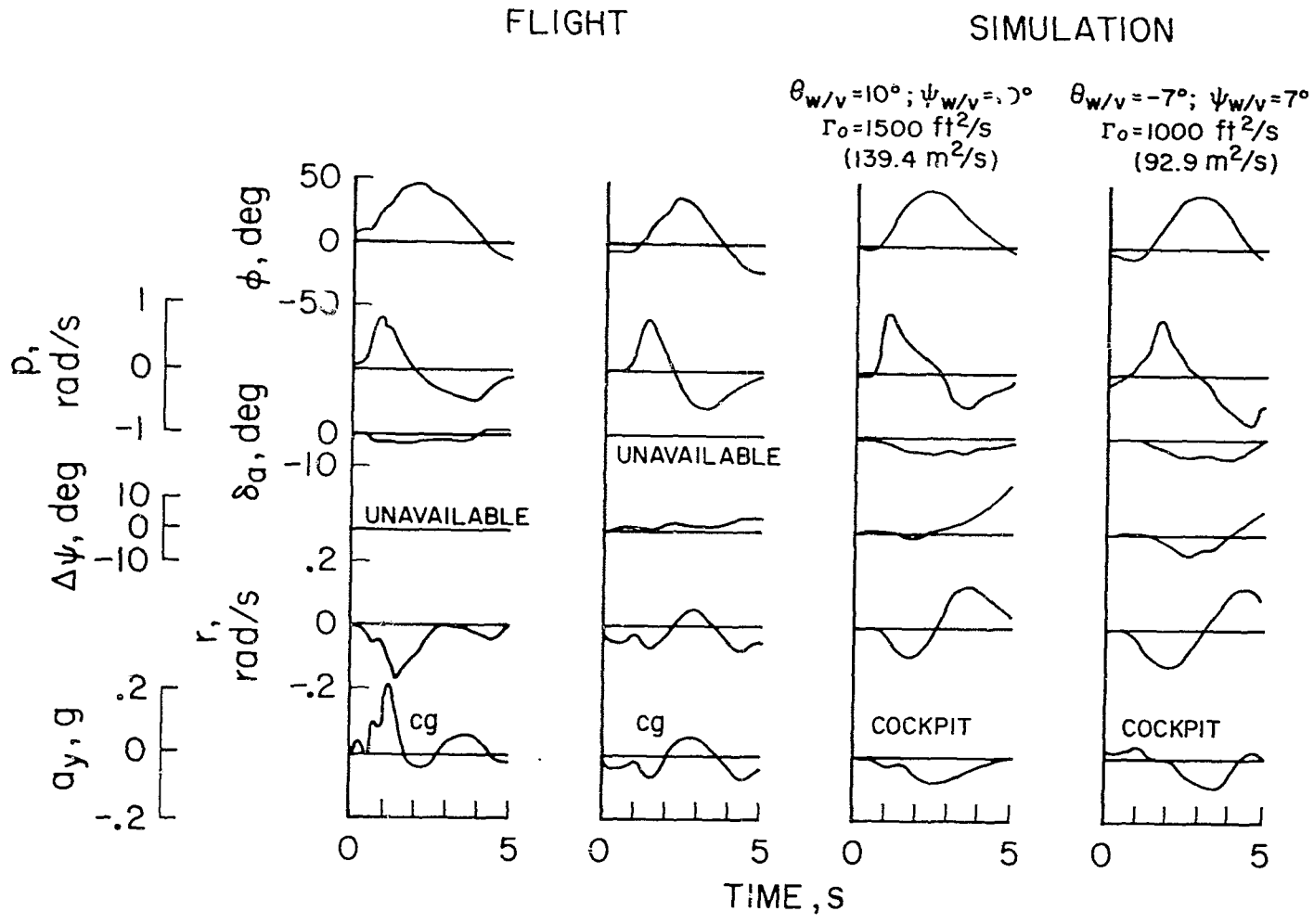

(a) Lateral characteristics.

Figure 6.— Comparison of flight and simulated encounters.

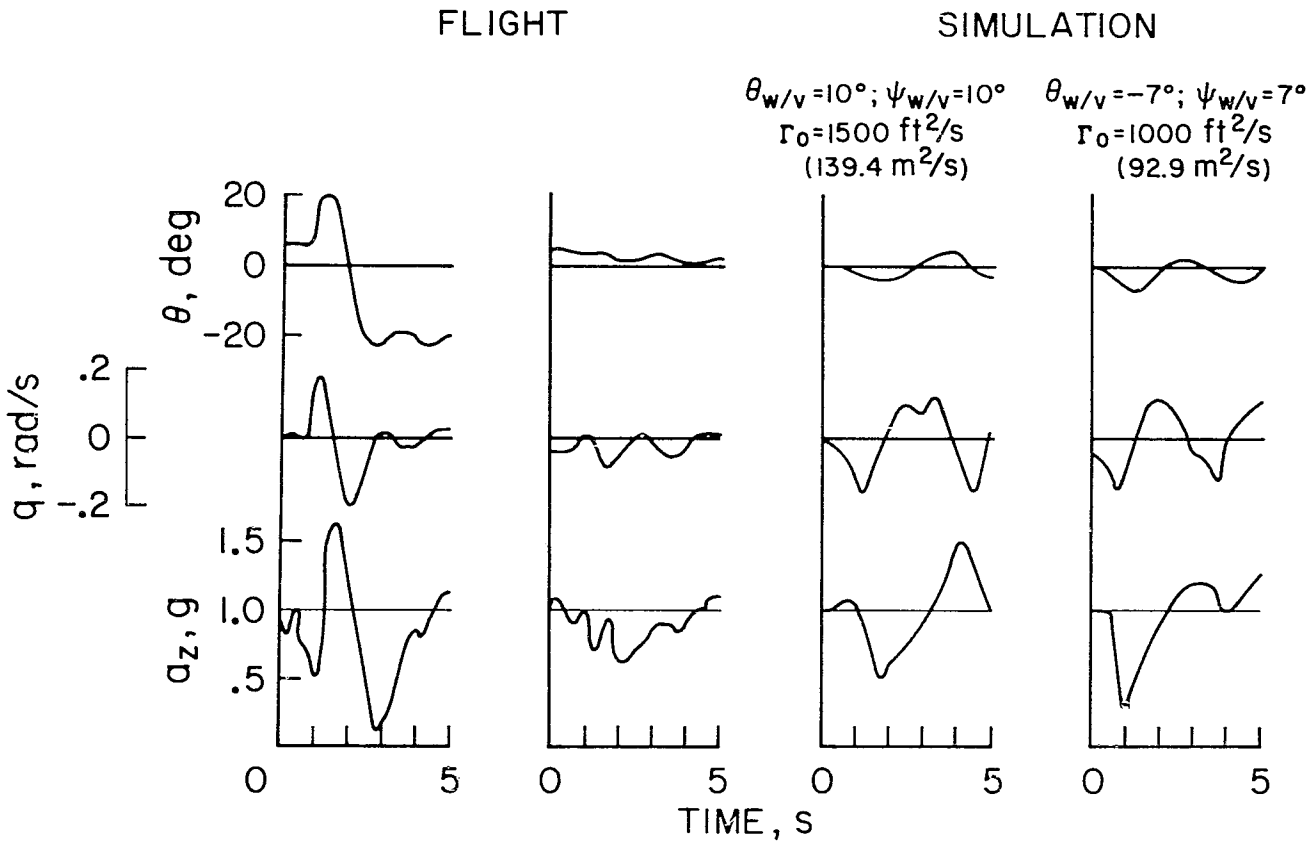

(b) Longitudinal characteristics.

Figure 6.— Concluded.

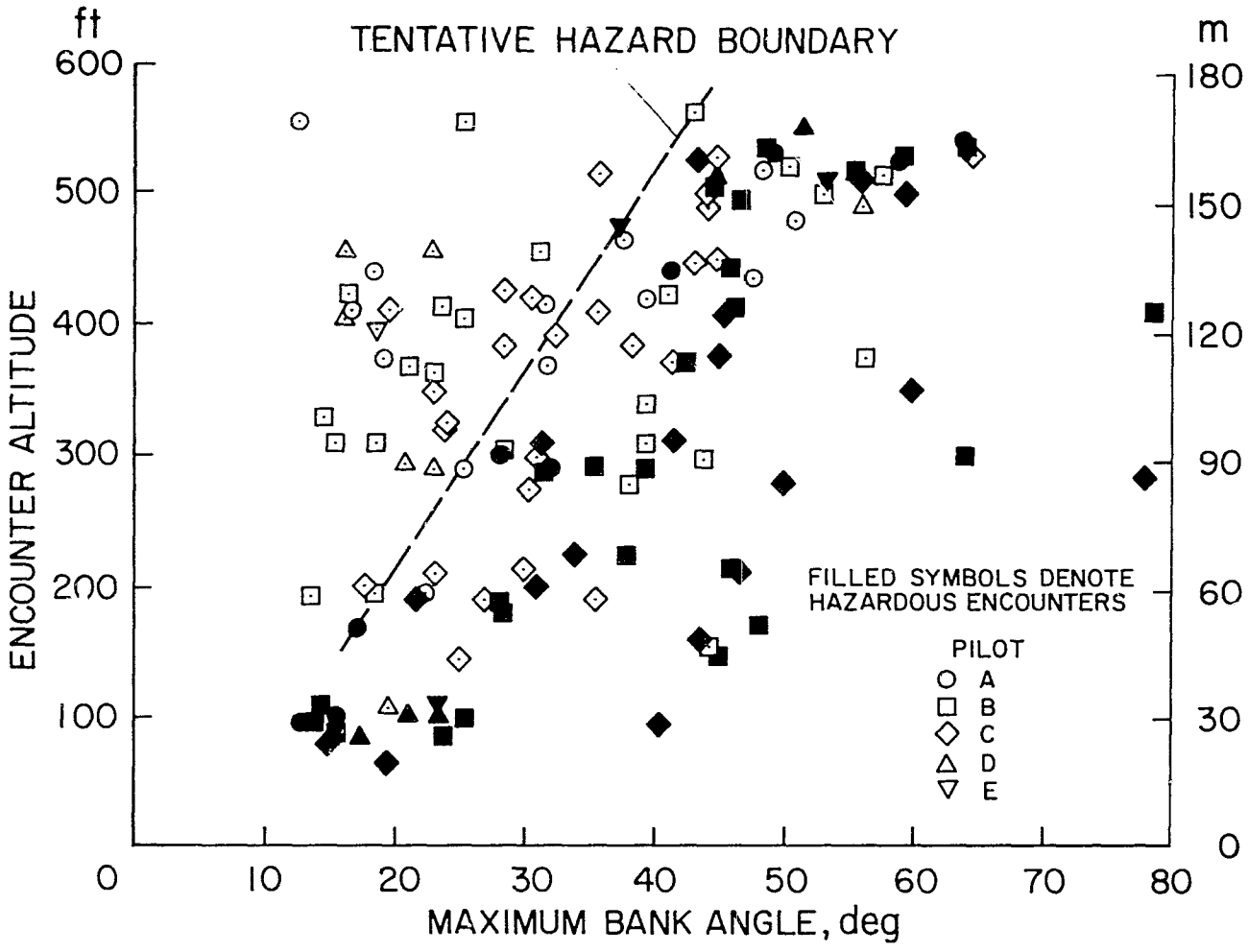

Figure 7.— Variation of encounter hazard with maximum bank angle and encounter altitude for all entry conditions, *VFR*.

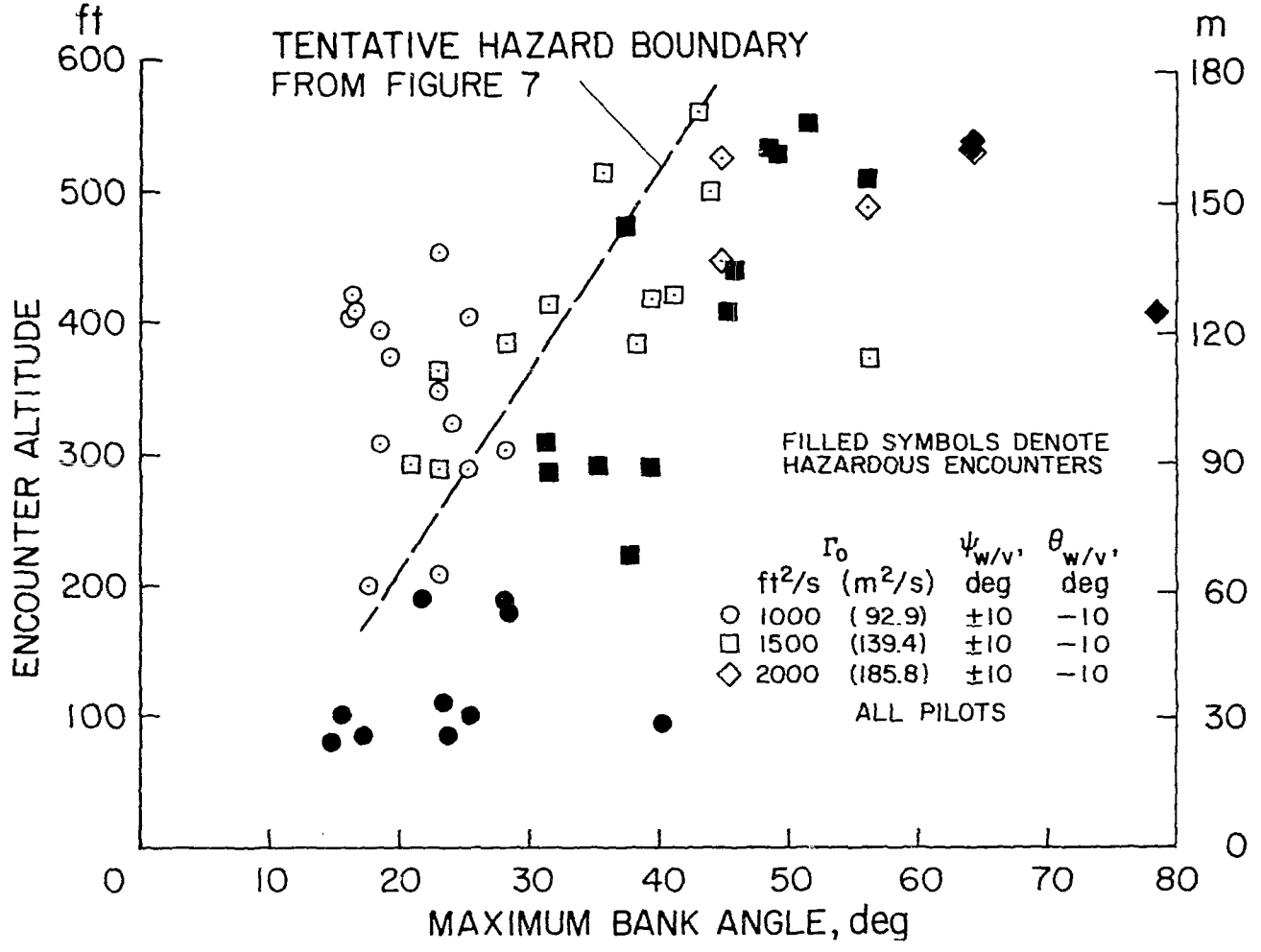

(a) Constant encounter angle.

Figure 8.— Variation of encounter hazard with maximum bank angle and encounter altitude, *VFR*.

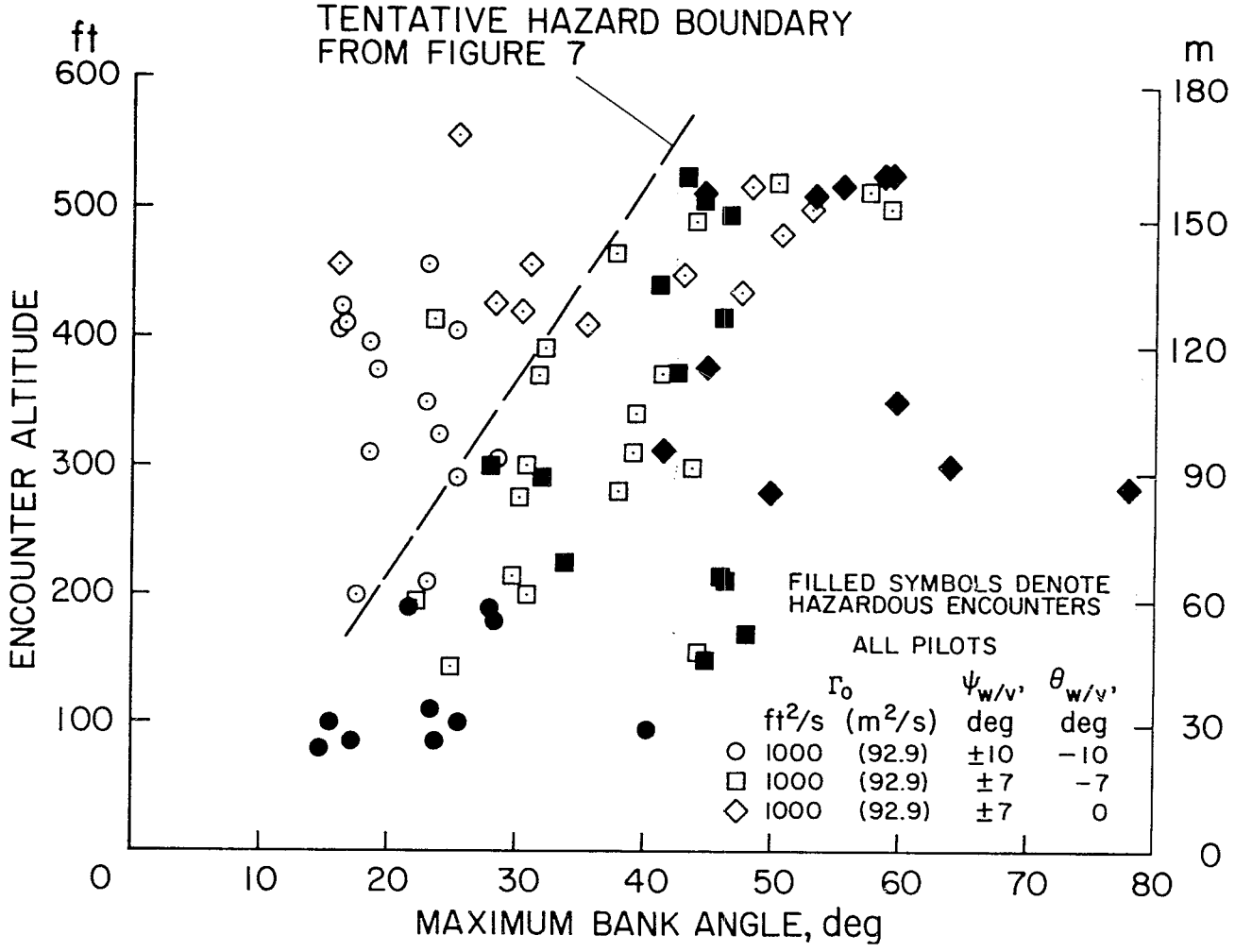

(b) Constant vortex strength.

Figure 8.— Concluded.

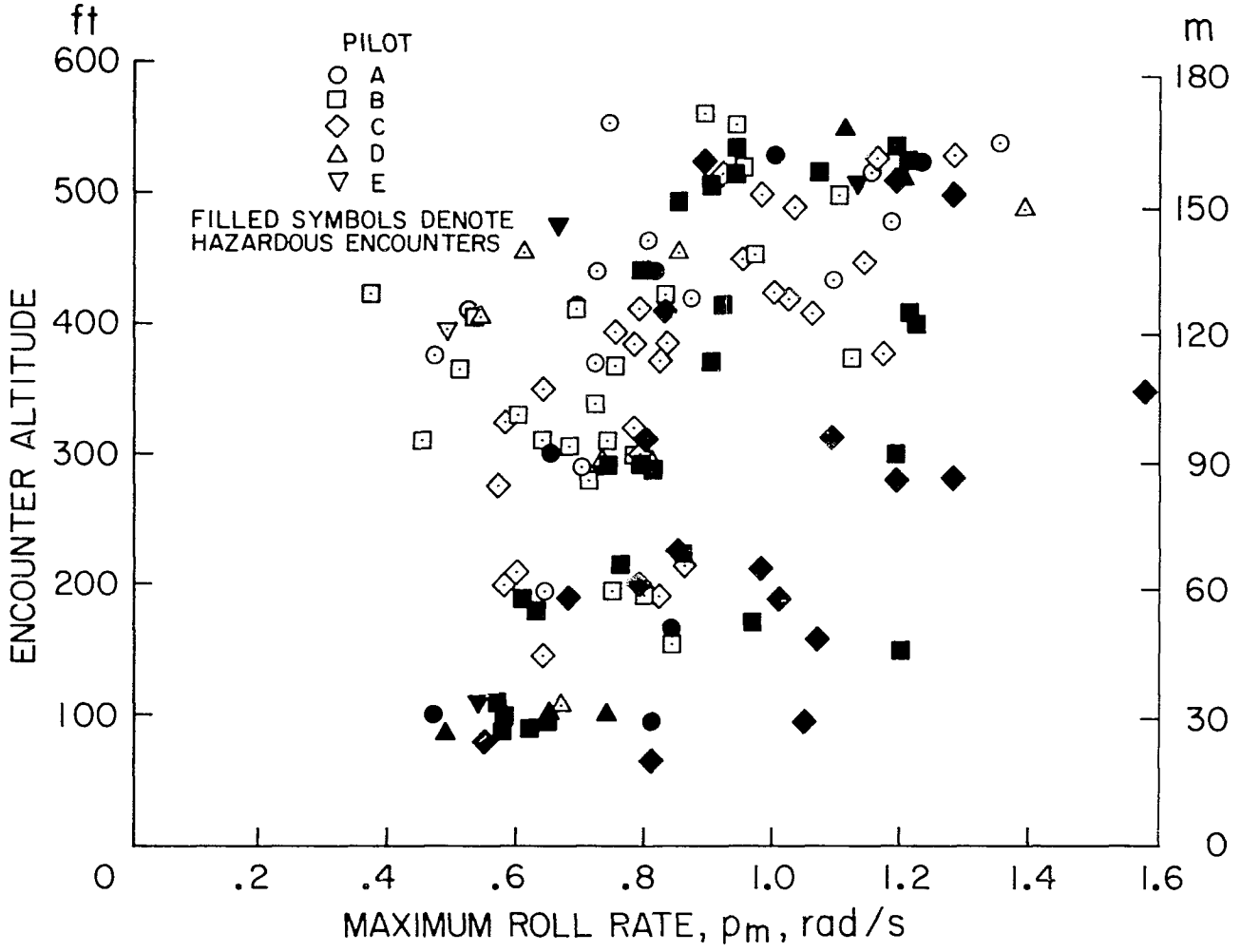

Figure 9.— Variation of encounter hazard with maximum roll rate and encounter altitude for all entry conditions, *VFR*.

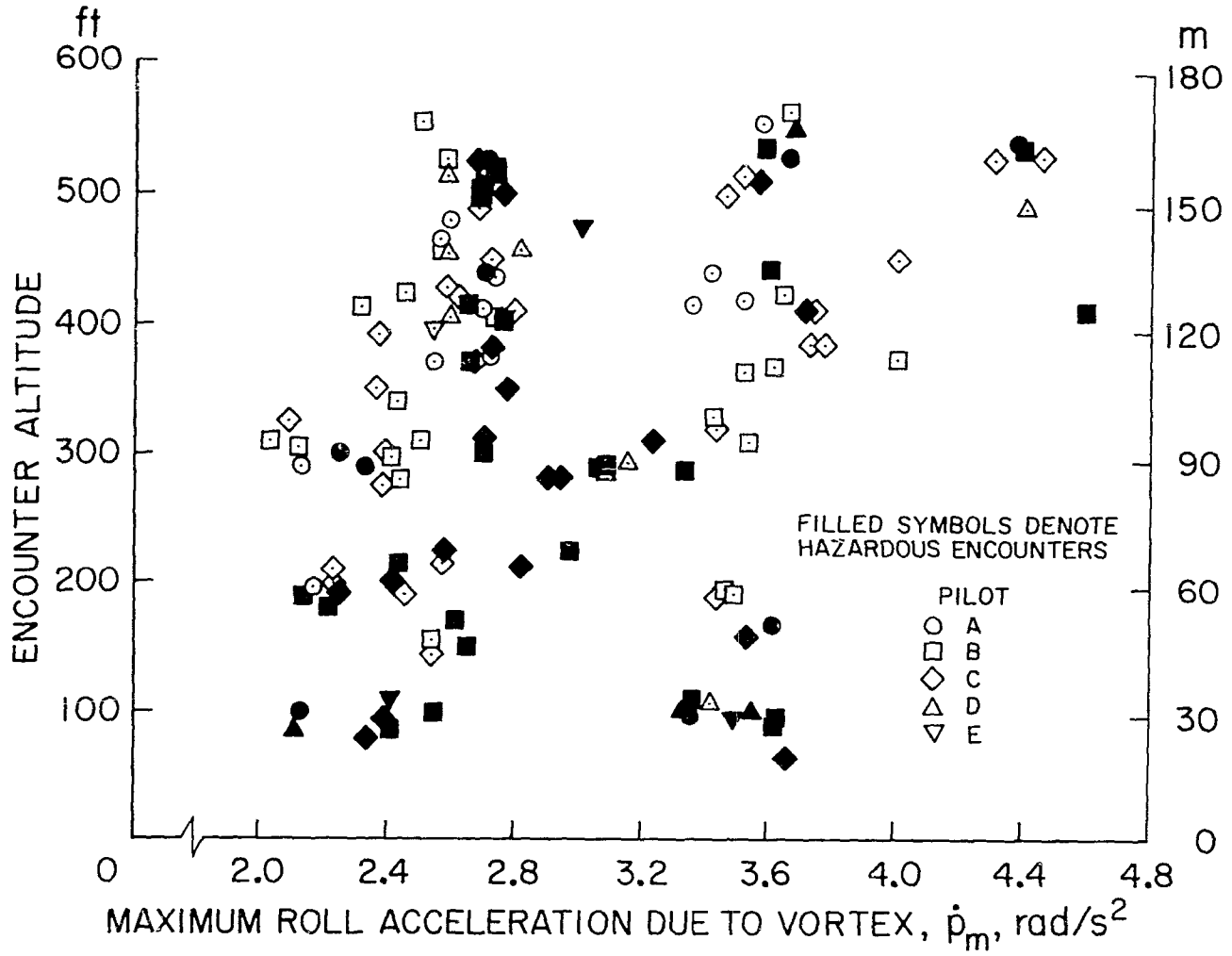

Figure 10.— Variation of encounter hazard with maximum roll acceleration due to the vortex and encounter altitude for all entry conditions, *VFR*.

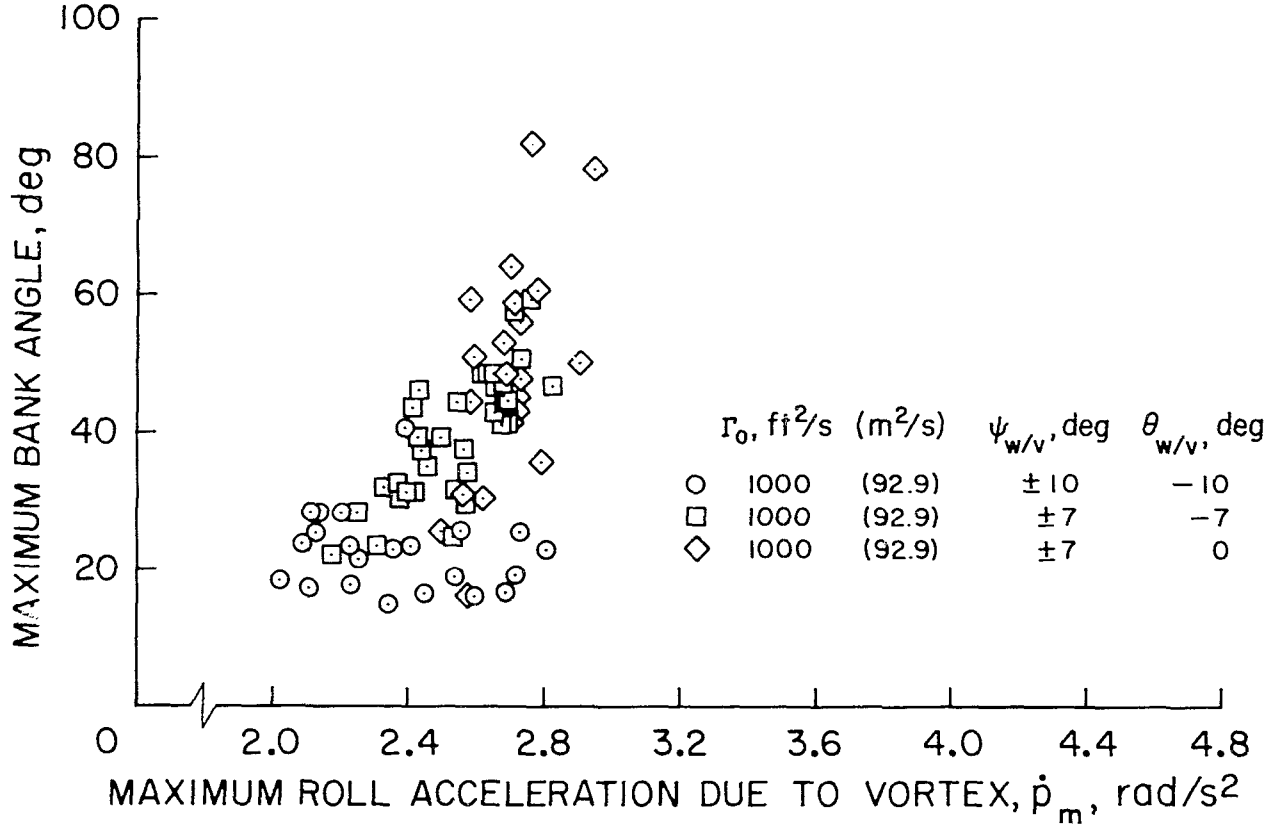

(a) Constant vortex strength.

Figure 11.— Variation of the maximum bank angle with the maximum roll acceleration due to the vortex.

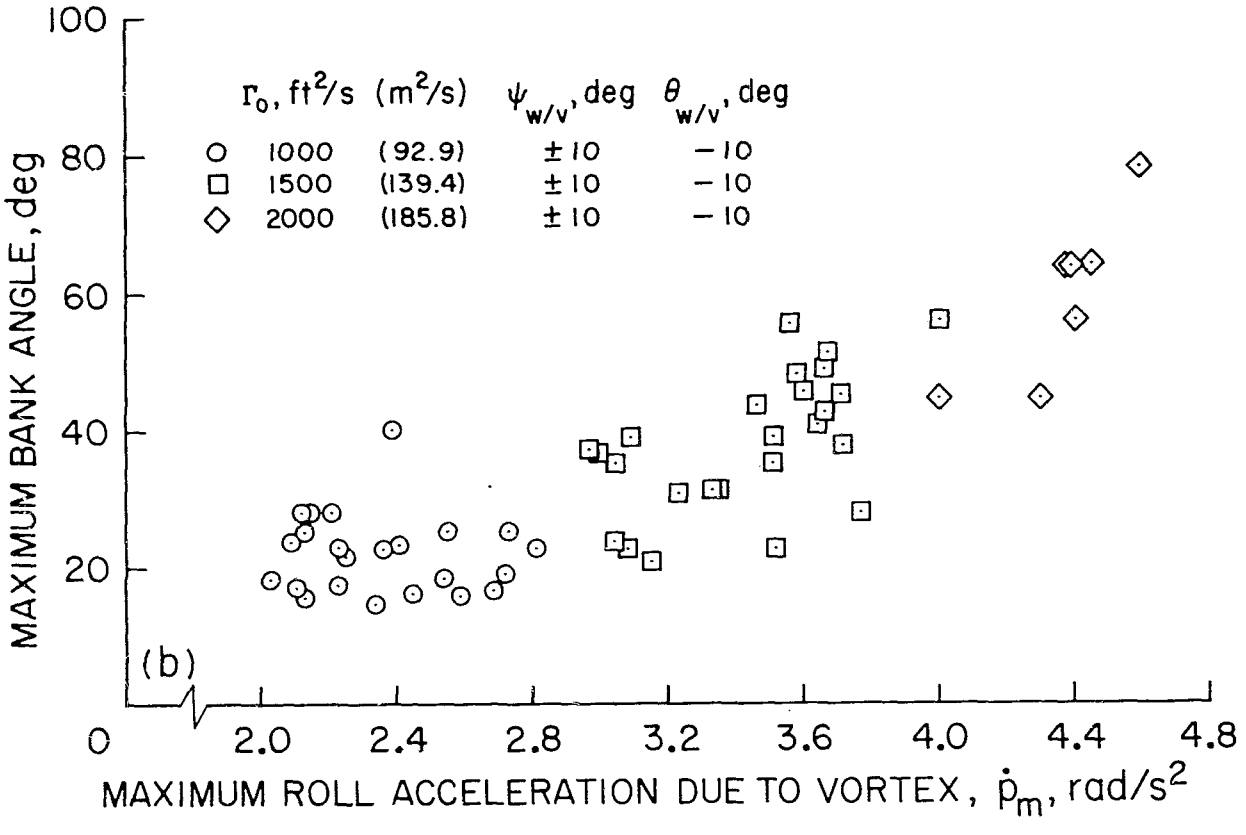

(b) Constant encounter angle.

Figure 11.— Concluded.

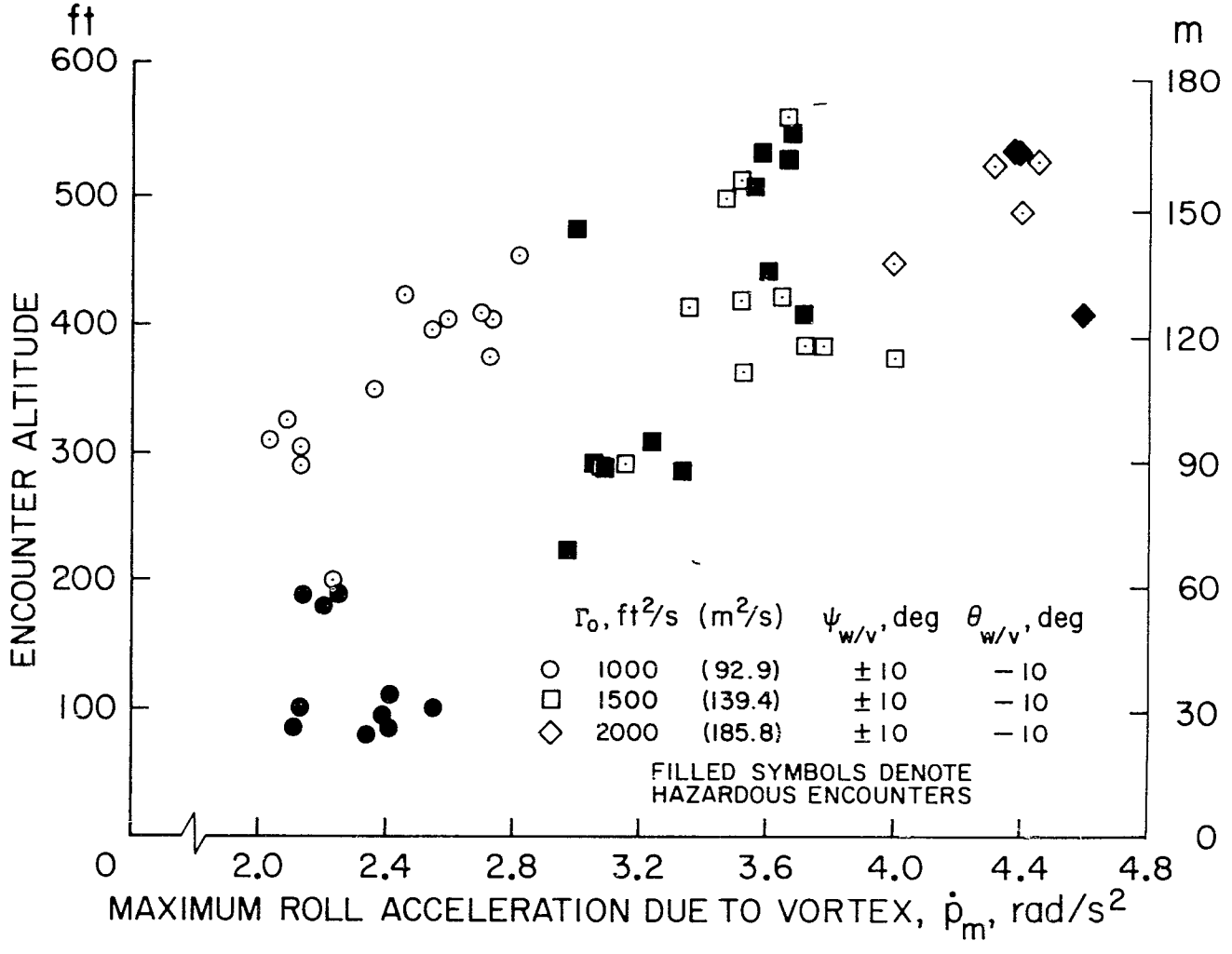

Figure 12.— Variation of encounter hazard with encounter altitude and maximum roll acceleration due to the vortex, *VFR*.

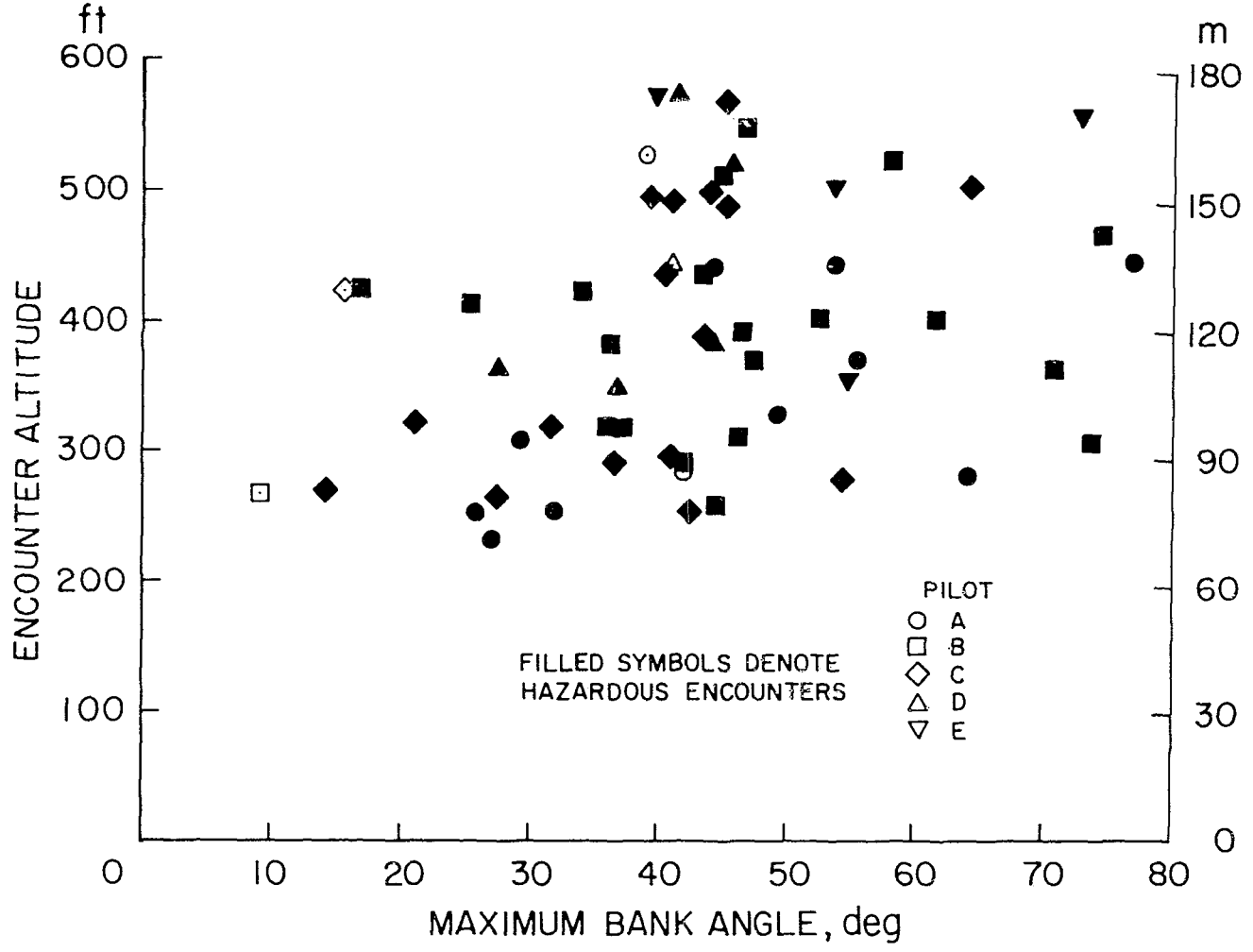

Figure 13.— Variation of encounter hazard with maximum bank angle and encounter altitude for all entry conditions, *IFR*.

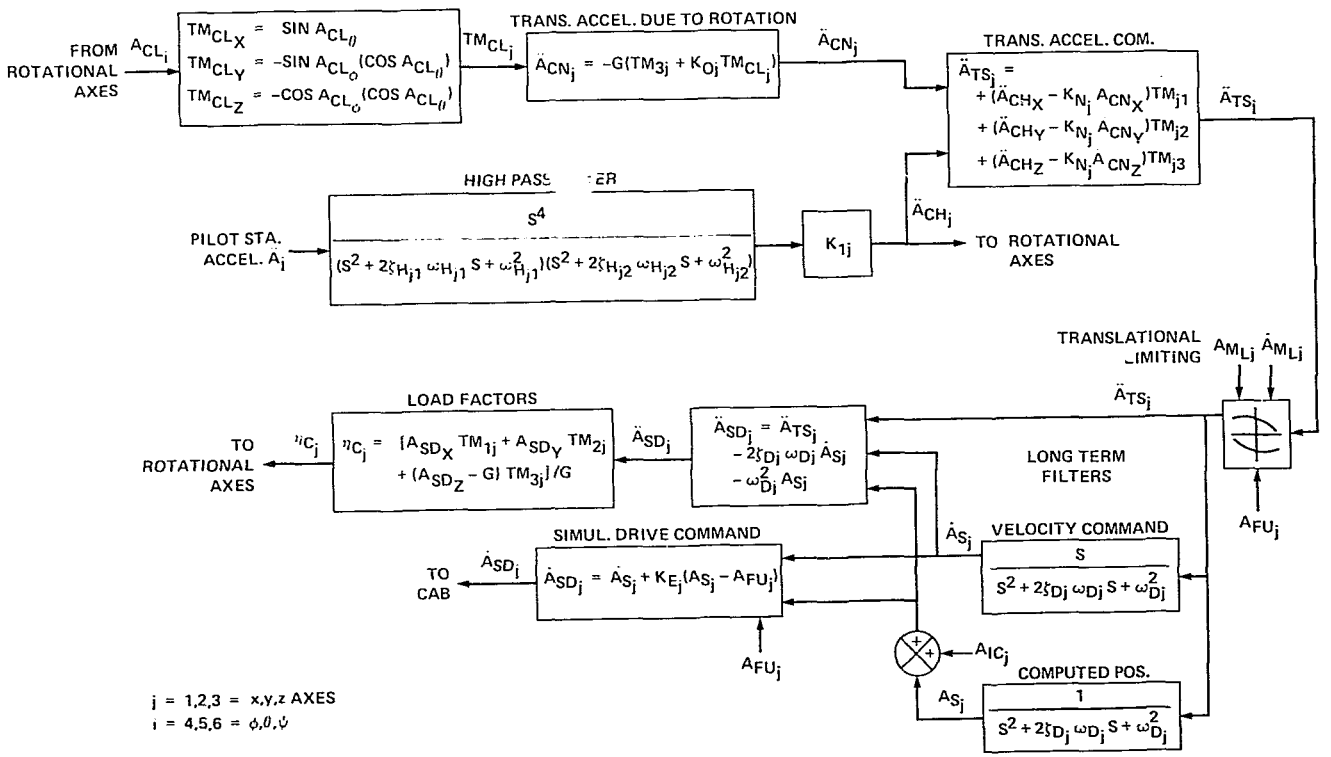

(a) Translational axes.

Figure 14.— Block diagram of washout motion system for S.01 simulator.

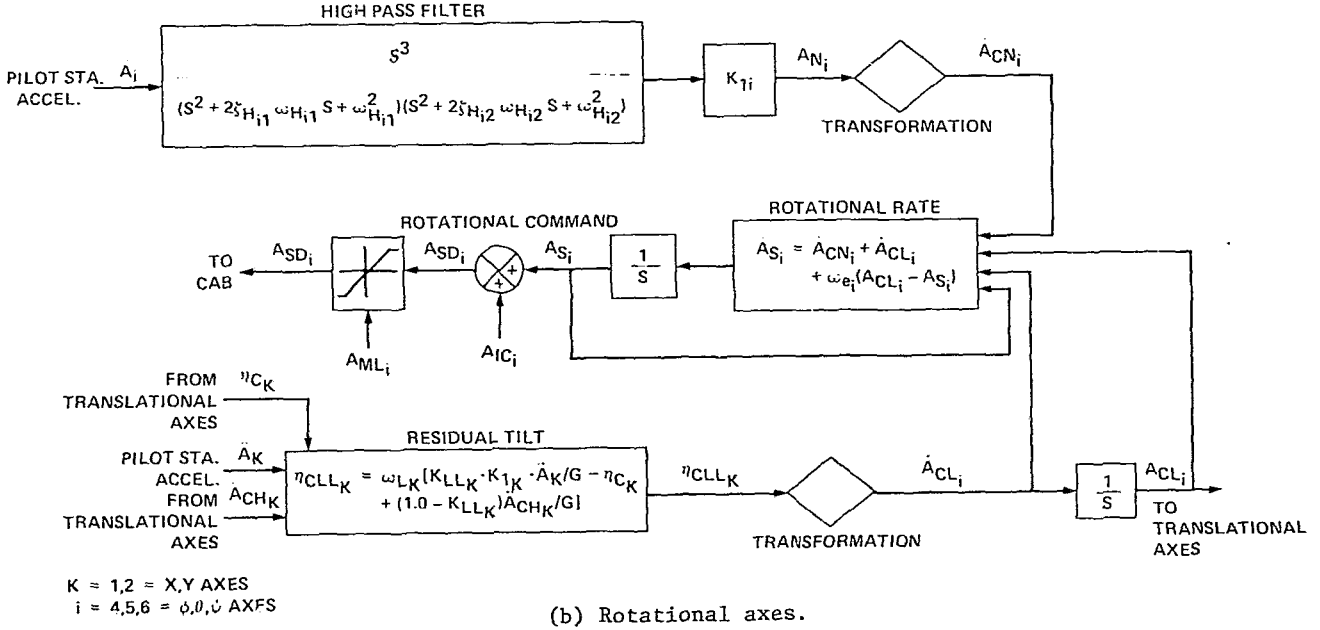

(b) Rotational axes.

Figure 14.— Concluded.

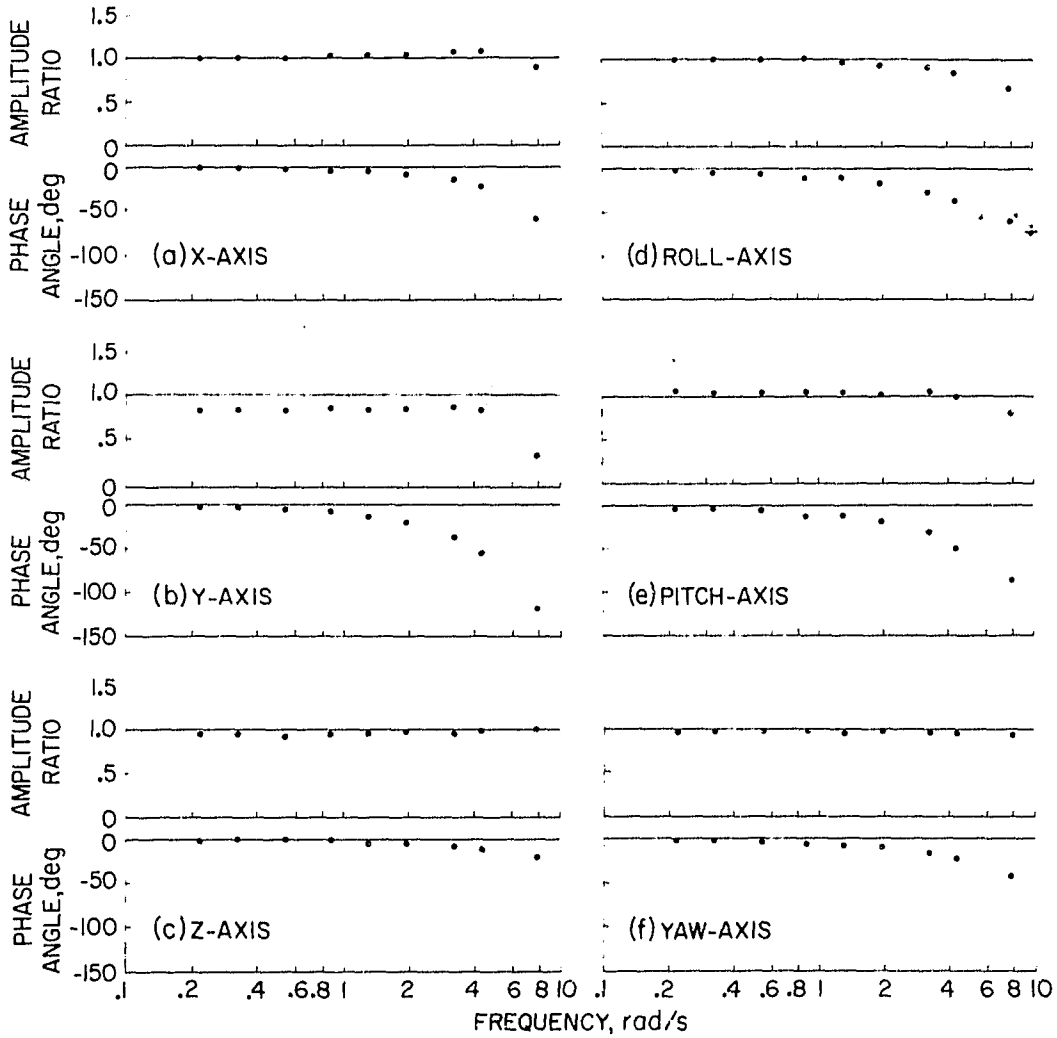

Figure 15.— Frequency response characteristics of S.01 simulator without washout.

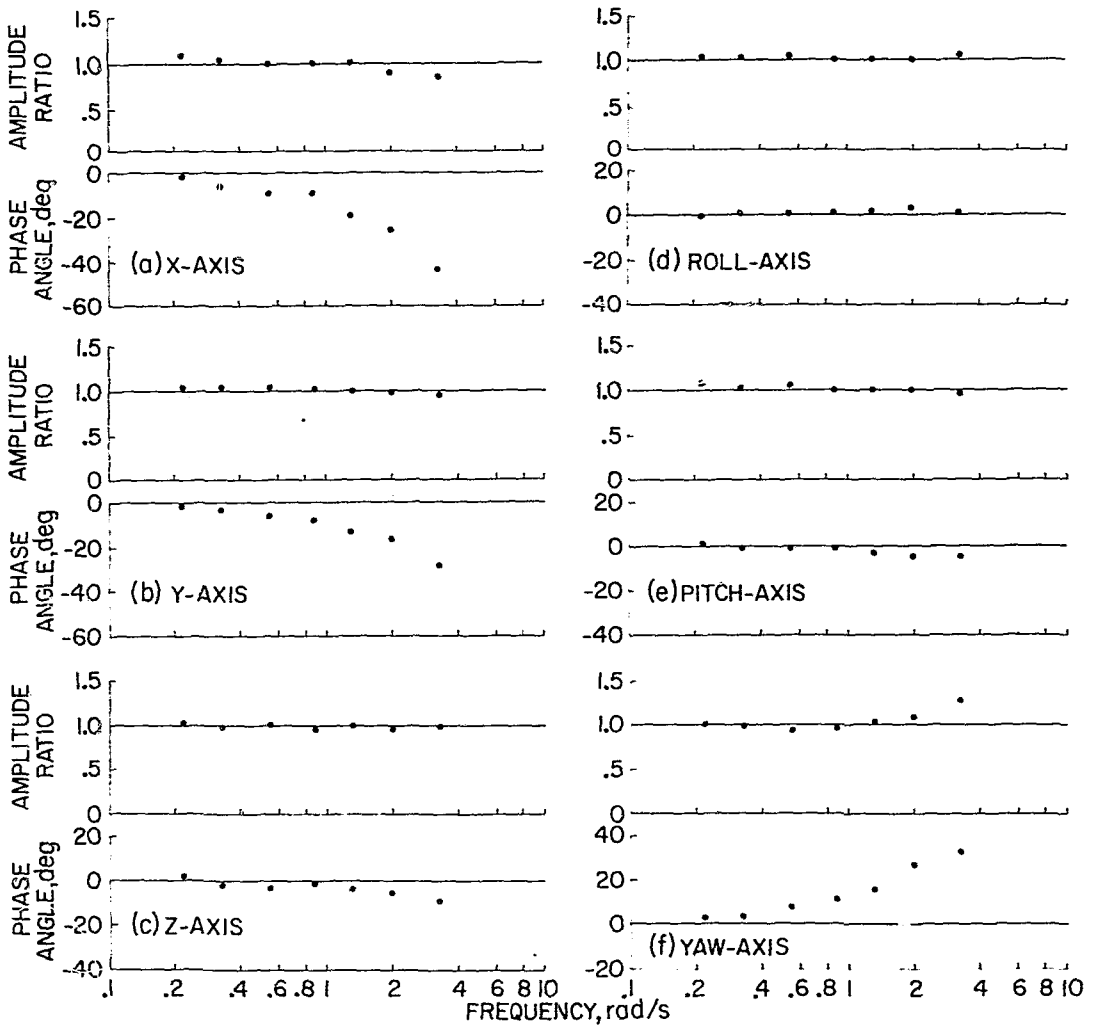

Figure 16.— Frequency response characteristics of the VFA.02 visual system.

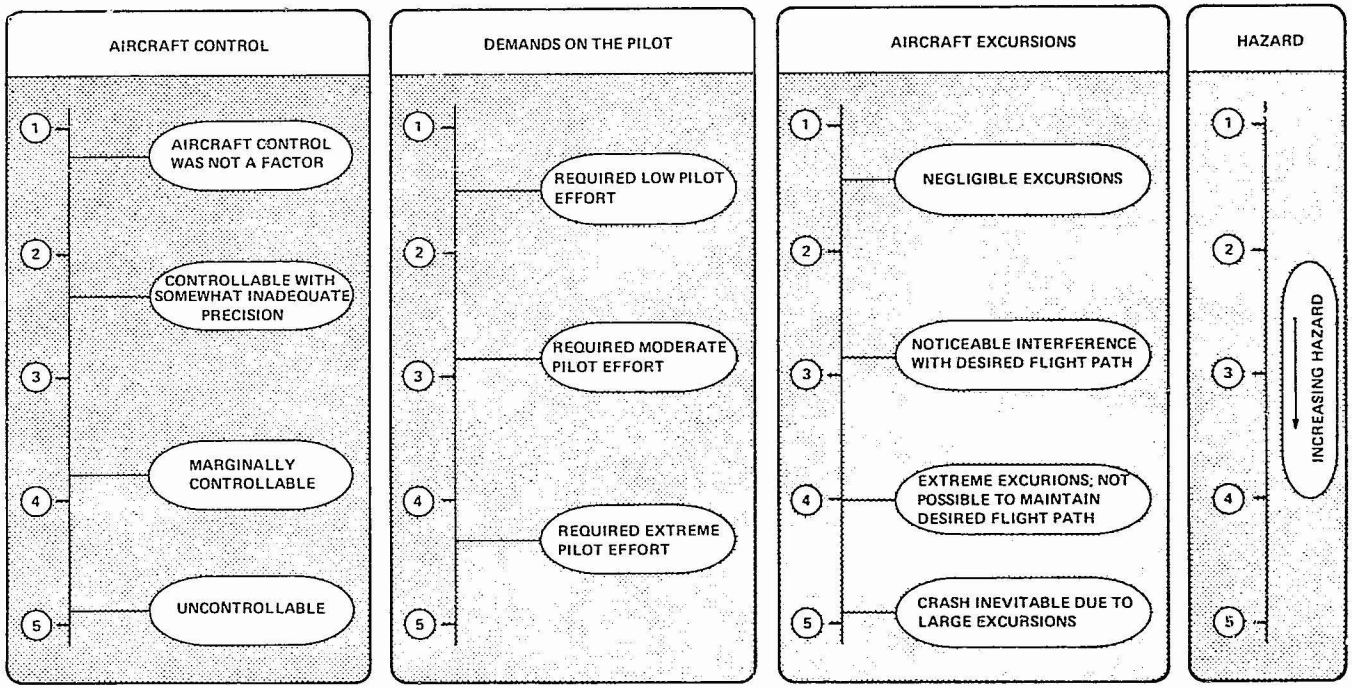

Figure 17.— Vortex hazard rating scale.

PILOT_____ DATE_____

RUN NUMBER_____

(1) Briefly describe the vortex encounter.

(2) Would you have continued on normal flight or aborted the task if this encounter occurred in flight?

(3) Did you consider the run hazardous?

(4) If the upset was deemed as hazardous, was the primary hazard:

- ☐ Ground impact?
- ☐ Structural failure due to vortex?
- ☐ Structural failure due to recovery attempt?

(5) Other comments:

Figure 18.— Pilot questionnaire.